Federal Highway Administration

100-Year Coating Study

PUBLICATION NO. FHWA-HRT-12-044

NOVEMBER 2012

U.S. Department of Transportation
Federal Highway Administration

Research, Development, and Technology
Turner-Fairbank Highway Research Center
6300 Georgetown Pike
McLean, VA 22101-2296

FOREWORD

The Federal Highway Administration 100-Year Coating Study was initiated in August 2009 to identify coating systems that can provide 100 years of virtually maintenance-free service life at comparable costs to the existing coating systems, even in adverse environments. Eight coating systems were selected for the study—three three-coat systems consisting of organic, inorganic, and moisture-cured zinc-based primers; four two-coat systems with various combinations of zinc-based primers and organic top coats; and a single-coat system of calcium sulfonate alkyd. One design innovation feature was the employment of 18- by 18-inch large test panels that contained welding joints and angle attachments using bolts and nuts to closely simulate realistic conditions that are encountered in bridges in the field. All coating systems were evaluated under accelerated laboratory testing and three outdoor exposure conditions, namely natural weathering and natural weathering with salt spray in McLean, VA, and outdoor testing at the Golden Gate Bridge in San Francisco, CA. This report presents results of the performance evaluation of the eight coating systems.

Jorge E. Pagán-Ortiz
Director, Office of Infrastructure
Research and Development

TECHNICAL REPORT DOCUMENTATION PAGE

1. Report No. FHWA-HRT-12-044	2. Government Accession No.	3. Recipient's Catalog No.
4. Title and Subtitle Federal Highway Administration 100-Year Coating Study		5. Report Date November 2012
		6. Performing Organization Code
7. Author(s) Pradeep Kodumuri (SES Group and Associates) and Seung-Kyoung Lee (Center for Advanced Infrastructure and Transportation)		8. Performing Organization Report No.
9. Performing Organization Name and Address SES Group and Associates 614 Biddle City Chesapeake City, MD 21915 (Formerly manager of FHWA Coatings and Corrosion Laboratory) Center for Advanced Infrastructure and Transportation Rutgers, the State University of New Jersey 100 Brett Road Piscataway, NJ 08854		10. Work Unit No. 11. Contract or Grant No.
12. Sponsoring Agency Name and Address Office of Infrastructure Research and Development Federal Highway Administration 6300 Georgetown Pike McLean, VA 22101-2296		13. Type of Report and Period Covered Final Report 14. Sponsoring Agency Code
15. Supplementary Notes The Federal Highway Administration project managers were Seung-Kyoung Lee (Rutgers) and Y.P.Virmani, HRDI-60.		
16. Abstract The Federal Highway Administration 100-Year Coating Study was initiated in August 2009 to search for durable coating systems at a reasonable cost. The objective of the study was to identify and evaluate coating materials that can provide 100 years of virtually maintenance-free service life for steel bridges. Selected coating systems included three three-coat systems, four two-coat systems, and a single-coat system of high-ratio calcium sulfonate alkyd. All coating systems were evaluated under accelerated laboratory testing and three outdoor exposure conditions, namely natural weathering and natural weathering with salt spray in McLean, VA, and outdoor testing at the Golden Gate Bridge in San Francisco, CA. One design innovation was the employment of 18- by 18-inch large test panels that contained welding joints and angle attachments using bolts and nuts to closely simulate realistic conditions that are encountered in bridges in the field. This report presents results of performance evaluation of the eight coating systems.		
17. Key Words One-coat, Two-coat, Three-coat, Steel bridge coatings, Corrosion protection, Accelerated laboratory testing, Outdoor exposure, Coating performance evaluation	18. Distribution Statement No restrictions. This document is available to the public through the National Technical Information Service, Springfield, VA 22161	

19. Security Classif. (of this report) Unclassified	20. Security Classif. (of this page) Unclassified	21. No of Pages 58	22. Price

Form DOT F 1700.7 (8-72) Reproduction of completed pages authorized.

SI* (MODERN METRIC) CONVERSION FACTORS

APPROXIMATE CONVERSIONS TO SI UNITS

Symbol	When You Know	Multiply By	To Find	Symbol
		LENGTH		
in	inches	25.4	millimeters	mm
ft	feet	0.305	meters	m
yd	yards	0.914	meters	m
mi	miles	1.61	kilometers	km
		AREA		
in^2	square inches	645.2	square millimeters	mm^2
ft^2	square feet	0.093	square meters	m^2
yd^2	square yard	0.836	square meters	m^2
ac	acres	0.405	hectares	ha
mi^2	square miles	2.59	square kilometers	km^2
		VOLUME		
fl oz	fluid ounces	29.57	milliliters	mL
gal	gallons	3.785	liters	L
ft^3	cubic feet	0.028	cubic meters	m^3
yd^3	cubic yards	0.765	cubic meters	m^3
	NOTE: volumes greater than 1000 L shall be shown in m^3			
		MASS		
oz	ounces	28.35	grams	g
lb	pounds	0.454	kilograms	kg
T	short tons (2000 lb)	0.907	megagrams (or "metric ton")	Mg (or "t")
		TEMPERATURE (exact degrees)		
°F	Fahrenheit	5 (F-32)/9 or (F-32)/1.8	Celsius	°C
		ILLUMINATION		
fc	foot-candles	10.76	lux	lx
fl	foot-Lamberts	3.426	$candela/m^2$	cd/m^2
		FORCE and PRESSURE or STRESS		
lbf	poundforce	4.45	newtons	N
lbf/in^2	poundforce per square inch	6.89	kilopascals	kPa

APPROXIMATE CONVERSIONS FROM SI UNITS

Symbol	When You Know	Multiply By	To Find	Symbol
		LENGTH		
mm	millimeters	0.039	inches	in
m	meters	3.28	feet	ft
m	meters	1.09	yards	yd
km	kilometers	0.621	miles	mi
		AREA		
mm^2	square millimeters	0.0016	square inches	in^2
m^2	square meters	10.764	square feet	ft^2
m^2	square meters	1.195	square yards	yd^2
ha	hectares	2.47	acres	ac
km^2	square kilometers	0.386	square miles	mi^2
		VOLUME		
mL	milliliters	0.034	fluid ounces	fl oz
L	liters	0.264	gallons	gal
m^3	cubic meters	35.314	cubic feet	ft^3
m^3	cubic meters	1.307	cubic yards	yd^3
		MASS		
g	grams	0.035	ounces	oz
kg	kilograms	2.202	pounds	lb
Mg (or "t")	megagrams (or "metric ton")	1.103	short tons (2000 lb)	T
		TEMPERATURE (exact degrees)		
°C	Celsius	1.8C+32	Fahrenheit	°F
		ILLUMINATION		
lx	lux	0.0929	foot-candles	fc
cd/m^2	$candela/m^2$	0.2919	foot-Lamberts	fl
		FORCE and PRESSURE or STRESS		
N	newtons	0.225	poundforce	lbf
kPa	kilopascals	0.145	poundforce per square inch	lbf/in^2

*SI is the symbol for the International System of Units. Appropriate rounding should be made to comply with Section 4 of ASTM E380.
(Revised March 2003)

TABLE OF CONTENTS

LIST OF FIGURES

LIST OF TABLES

CHAPTER 1. INTRODUCTION

The coating industry switched from lead-based to zinc-based three-coat systems in the 1970s due to health hazards associated with lead in the coatings to protect steel bridges from corrosion.[1] The current state of practice in steel bridge coatings usually involves multi-layer coating typically consisting of a zinc-rich primer over an abrasive blast-cleaned surface and one or two additional coating layers on top of the primer. Both inorganic and organic zinc-rich primers provide galvanic corrosion protection by sacrificing itself to the less electrochemically active steel substrate in the presence of corrosive conditions. The intermediate coat provides a physical barrier to the passage of moisture, oxygen, and other aggressive ions, such as chloride ions, while the top coat protects underlying coating layers against deterioration caused by ultraviolet (UV) radiation and physical damage and enhances the aesthetics of the coating system. It was reported that some three-coat systems with zinc-rich primers can have a service life up to 30 years of protecting steel from corrosion before a major touch-up is required.[2]

Typical costs for conventional coating systems include costs associated with removing mill scale and creating adequate surface condition, coating application, and logistics of moving coated steel bridge members to the field. Such shop operations also require downtime and space during the application of multiple coating layers. The high cost of mill scale removal and surface preparation can be attributed primarily to expensive open-blast cleaning equipment and labor.[2] The cost of typical three-coat systems ranges from under 4 percent to more than 24 percent of the cost of fabricating the steel.[3] After the first shop application, repainting the same bridge after approximately 30 years is very expensive. A practical alternative in reducing these repetitive coating costs is to extend the service life of the shop-applied original steel bridge coatings.[2]

The Federal Highway Administration (FHWA) Coatings and Corrosion Laboratory at the Turner-Fairbank Highway Research Center (TFHRC) initiated an in-house study in August 2009 to identify coating systems that can provide 100 years of virtually maintenance-free service life at comparable costs to the existing coating systems, even in adverse environments. Coating systems in this research study were selected based on past experience and results from previous FHWA studies that evaluated coating systems such as moisture-cured urethanes, waterborne acrylic and epoxy systems, two-coat systems, and one-coat systems. (See references 4–8.) Particularly, previous FHWA in-house studies indicate that the two-coat systems may perform well relative to the well-performing legacy zinc-rich three-coat systems. While critical factors in the field include being cost effective due to a lower number of coats and having reduced application time, two-coat systems have the potential to replace the conventional three-coat systems without sacrificing corrosion protection properties.[9] This report presents research findings from a performance evaluation of eight coating systems based on experimental data from accelerated laboratory testing (ALT) and outdoor exposure testing.

CHAPTER 2. EXPERIMENTAL PROCEDURES

2.1 SELECTION OF COATING SYSTEMS

Table 1 summarizes the eight coating systems employed in this study. Two three-coat systems were used as controls, and the remaining coating systems were test systems composed of a three-coat system, four two-coat systems, and a one-coat system. The acronyms used for all the coating systems are listed in the table. The coating systems will be identified using these acronyms throughout the report.

Table 1. Summary of coating systems.

System Number	System ID	Coating Type		
		Primer	Intermediate	Top
1	Three-coat (control)	Inorganic zinc-rich epoxy (IOZ)	Epoxy (E)	Aliphatic polyurethane (PU)
2		Zinc-rich epoxy primer (ZE)	E	PU
3	Three-coat	Moisture-cured urethane zinc primer (MCU)	E	Fluorourethane (F)
4	Two-coat	ZE		PU
5		Inorganic zinc primer (Zn)		Polysiloxane (PS)
6		Thermally sprayed zinc primer (TSZ)		linear epoxy (LE)
7		Experimental zinc primer (ZnE)		LE
8	One-coat	High-ratio calcium sulfonate alkyd (HRCSA)		

2.2 PREPARATION OF TEST PANELS

All of the coating systems were applied onto steel substrates prepared according to the Society for Protective Coatings (SSPC) surface preparation standard number 5 (white metal blast) condition.[10] Subsequently, individual coating systems were applied on the cleaned test panels using an airless spray method by a professional coating laboratory.

Conventional test panels (type I) used for previous FHWA in-house coating studies were 4 by 6 inches. For this study, a new type of test panel (type II) was designed in addition to the conventional test panels to closely simulate detailing of steel bridge members. Each of the type II panels was 18 by 18 inches and contained “V”-shaped and inverted “T”-shaped welding joints, an overlap joint, an angle attachment, and five bolt-nut assemblies, as shown in figure 1 and figure 2. In this report, all type II base plates and individual components were separately spray coated with the primer before panel assembly. After the primer was allowed to dry for 24 h, the components were assembled and coated with an intermediate coat and/or top coat. Introduction of complex geometry to the panel design was employed to understand how coatings applied over

the crevices and interfaces created by the attachments, nuts, and bolts of the type II panel perform compared to those applied on the small type I flat panels.

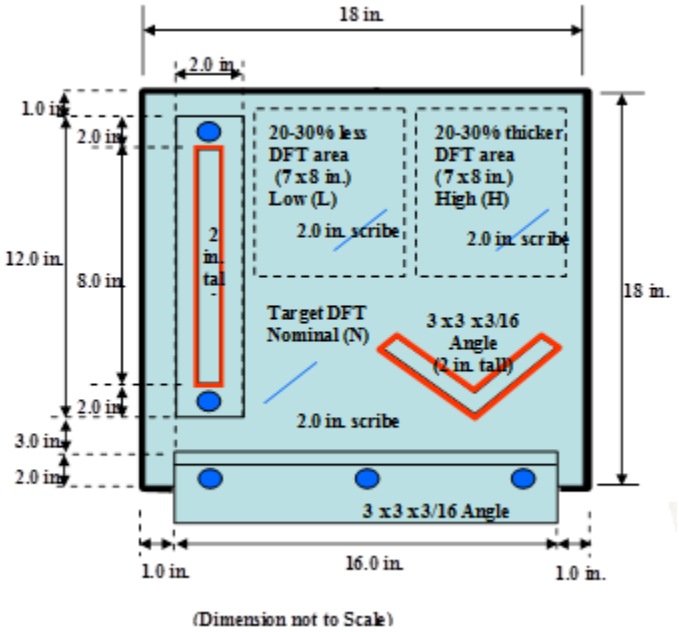

Figure 1. Illustration. Type II test panel.

Figure 2. Photo. Images of type II test panels.

All type I test panels were coated according to manufacturers' dry film thickness (DFT) recommendations. Each type II panel consisted of three coated areas with the following varying DFT values:

- **Nominal DFT (N)**: Target DFT recommended by the manufacturers.
- **Low DFT (L)**: DFT 20 percent less than the target DFT.
- **High DFT (H)**: DFT 20 percent higher than the target DFT.

Test results from these three DFT areas revealed how much DFT of a particular coating system influenced coating performance. The physical locations of these test areas on the surface of the type II test panel are shown in figure 1.

A total of 100 type I and 27 type II test panels were prepared for ALT and outdoor exposure testing. Table 2 and table 3 list the exposure condition and number for type I and II panels, respectively. Outdoor exposure tests were performed in the backyard of TFHRC in McLean, VA, and at the Golden Gate Bridge (GGB) in San Francisco, CA. The TFHRC exposure testing consisted of natural weathering (NW) and natural weathering with daily salt spray (NWS).

For type I test panels, each coating system was sprayed on 12 panels, where 5 panels were used for ALT (three scribed and two unscribed), 5 panels were used for NW (one scribed and one unscribed) and NWS (two scribed and one unscribed), and 2 panels were used for physical tests of adhesion strength and Fourier transform infrared spectroscopy (FTIR). In addition, two uncoated type I steel panels were deployed on each of the TFHRC outdoor exposure racks.

For type II panels, three panels per coating system were used, one each for the NW and NWS racks at TFHRC and the third one on the GGB rack. Also, an uncoated type II panel was exposed on each of three exposure racks. The overall test matrix of type II panels is provided in table 3.

Table 2. Number of exposure conditions for type I test panels.

Group	Number of Coating Systems	ALT	Outdoor Tests		Physical Testing	Total Number of Test Panels
			NW	NWS		
Uncoated steel	N/A	N/A	2	2	N/A	4
Control	2	10	5	5	4	24
Test coating systems	6	30	18	12	12	72
Subtotal	8	40	25	19	16	100

N/A = Not applicable since uncoated steel panels were not tested in ALT and were not used for physical testing.

Table 3. Number of exposure conditions for type II test panels.

Group	Number of Coating Systems	Outdoor Tests			Total Number of Test Panels
		NW	NWS	GGB	
Uncoated steel	N/A	1	1	1	3
Control	2	2	2	2	6
Test coating systems	6	6	6	6	18
Subtotal	8	9	9	9	27

N/A = Not applicable since no coating systems were applied on uncoated steel.

After the test panels were delivered to TFHRC, their as-received condition was documented, and six type I panels (three for ALT and three for outdoor testing) for each coating system were scribed following the instructions specified in ASTM D1654-08, "Standard Test Method for Evaluation of Painted or Coated Specimens Subjected to Corrosive Environments."[(11)] A 2-inch-long scribe was made diagonally on each panel using a mechanical scriber shown in figure 3.

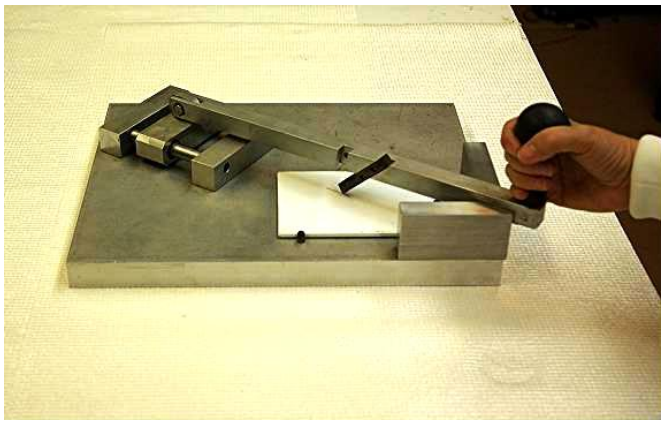

Figure 3. Photo. Scribing tool.

All test areas of type II test panels were scribed. A mechanical scribing tool used for type I panels was not suited for the large-size test panels. As a result, the test areas were scribed manually using a high-speed Dremel® tool with a scribing bit, as shown in figure 4. C-clamps were used to support a metallic guide along which the scribing was done.

Figure 4. Photo. Dremel® scribing tool.

Initial trial scribes were made on dummy test panels to optimize the speed of rotation of the Dremel® bit and applied pressure. The pattern (depth and width) of the scribe made on the dummy test panels was examined using a handheld optical microscope. From this trial, operational parameters were finalized to obtain the ASTM D1654-08 specified width and depth of the scribe, and actual scribes were made on all of the type II panels.[(11)]

2.3 TEST CONDITIONS

ALT

Table 4 summarizes the test conditions for ALT and the total number of cycles. Each ALT cycle was carried out for 360 h, and a total of 20 cycles were planned. Upon completion of every cycle, the panels were examined for their performance. The test panels were also evaluated at the termination of ALT.

Detailed description of each 360-h test cycle is as follows:

- Freeze: 24 h.
- Temperature: -10 °F.
- UV/condensation: 168 h (7 days).
- Test cycle: 4-h UV/4-h condensation cycle.
- UV lamp: UVA-340 nm (wavelength recommended for UV tests).
- UV temperature: 140 °F.
- Condensation temperature: 104 °F.
- Prohesion (cyclic salt-fog, ASTM G85-11, "Standard Practice for Modified Salt Spray (Fog) Testing"): 168 h (7 days).[12]
- Test cycle: 1 h wet/1 h dry.
- Wet cycle: A Harrison mixture of 0.35 weight (wt) percent ammonium sulfate and 0.5 wt percent sodium chloride was used. Fog was introduced at ambient temperature.
- Dry cycle: Air was preheated to 95 °F and was then purged to the test chamber.

Table 4. ALT of type I panels.

Item	Freeze Exposure (hours)	UV Condensation Exposure (hours)	Prohesion Exposure (hours)	Total Exposure (hours)
Each cycle	24	168	168	360
Target duration (20 cycles)	480	3,360	3,360	7,200

Figure 5 and figure 6 show a salt fog chamber and a weathering tester, respectively. A 16-h salt-fog accumulation test was conducted before each cyclic salt-fog test to check the atomizing and fog quantity as well as the pH of the collected solution. Typical collection volume of the accumulation test was 0.034–0.068 oz/h, with uniform accumulation in all collection vessels placed at the four corners of the salt-fog chamber and at the center a few feet away from the spray nozzle. Pump speed, throw pressure, and flow rate were adjusted to optimize the collection volume.

Figure 5. Photo. Salt-fog chamber.

Figure 6. Photo. UV weathering tester.

Outdoor Exposure Testing at TFHRC

Type I and II test panels were deployed on two wooden racks inclined at 30 degrees facing south in the backyard at TFHRC in McLean, VA, as shown in figure 7 and figure 8.

Figure 7. Photo. NWS rack at TFHRC.

Figure 8. Photo. NW rack at TFHRC.

In the beginning of the study, NWS test panels received salt spray manually once a day, 5 days per week. Later, an automated daily salt spray system was designed and installed on the NWS rack as shown in figure 9 using the following components:

- 15 wt percent aqueous sodium chloride solution.
- Storage tank for the salt solution (30 gal).
- Electromechanical pump operating in combination with a timer that switches on for a specific time period at a specific time of the day.
- Tubing/piping required for salt solution to flow through to spray onto the deployed panels and a wooden rack.
- Shower heads to spray salt solution onto the deployed panels.

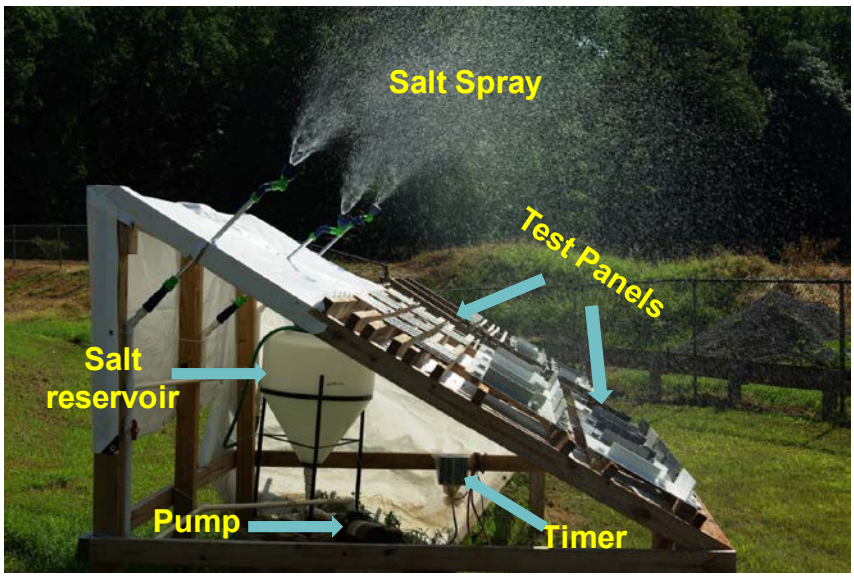

Figure 9. Photo. Automated salt spray system for NWS at TFHRC.

The automated salt spray system provided benefits such as eliminating the need to manually spraying the panels while uniformly spraying all the panels. As a result, daily salt spray could be carried out on weekends and holidays without human intervention. The timer turned the pump on for 15 s of salt spray at 10 a.m. each day. After a week of salt spray, it was clear that the 15 wt percent solution was too severe. Therefore, the salt solution was changed to the Harrison mixture (0.35 wt percent ammonium sulfate and 0.5 wt percent sodium chloride), which was the same solution employed in ALT. Digital pictures of test panels on the racks were recorded every month, and test panels were evaluated for coating performance after 6 months and again at 10 months at the project termination.

Outdoor Exposure Testing at GGB

The outdoor exposure condition at GGB was considered extremely harsh due to severe fog conditions containing airborne chlorides. Figure 10 shows type II panels deployed on top of the south anchorage house near the south abutment. Test panels were scheduled to be evaluated every 6 months for coating performance.

Figure 10. Photo. Type II panels deployed at GGB.

2.4 COATING CHARACTERIZATION TESTS AND PERFORMANCE EVALUATION TECHNIQUES

A series of characterization tests were conducted on the test panels before, during, and after ALT and outdoor exposure tests. Baseline data of DFT, color, gloss, adhesion, and coating defects were collected for each coating system prior to the scheduled tests. Performance of these coating systems was evaluated in terms of development of surface defects and rust creepage during the tests and soon after the completion of the tests. Changes in color, gloss, and adhesion strength were evaluated at the termination of testing. A digital microscope and a digital camera were also employed to document appearance changes of the test panels throughout the study. In addition, electrochemical impedance spectroscopy (EIS) was used to quantify change of coating barrier properties in terms of coating impedance.

DFT

The mean DFT of a coating system was measured in three spots for each type I panel before ALT and outdoor exposure testing using an electronic thickness gauge according to SSPC paint application specification 2, *Measurement of Dry Coating Thickness with Magnetic Gages*.[13] In addition, three spots per each DFT area on the type II panels were obtained to record actual DFTs in each panel.

Gloss

Gloss is defined as the perception of a shiny surface by human eyes. Specular gloss compares the luminous reflectance of a test specimen to that of a standard specimen under the same geometric conditions.[14] Measurements by this test method correlate with visual observations of surface shininess made at roughly the corresponding angles. Measured gloss ratings are obtained by comparing the specular reflectance from the specimen to that from a black glass standard. The

measured gloss ratings change as the surface refractive index changes since specular reflectance depends on the surface refractive index of the specimen.

Gloss of all of the coating systems was measured following ASTM D523-08, "Standard Test Method for Specular Gloss."[15] The 60-degree geometry measurements were conducted on the selected unscribed test panels before and after ALT and outdoor exposure tests. Three gloss readings for each type I panel and six readings for each type II panel were recorded. The reported gloss of each coating system per test condition was the mean of the readings obtained from all unscribed test panels.

Color

The color of the coatings was measured using a colorimeter following ASTM D2244-05, "Standard Practice for Calculation of Color Tolerances and Color Differences from Instrumentally Measured Color Coordinates."[16] This technique is based on the calculation from instrumentally measured color coordinates based on daylight illumination, color tolerances, and small color differences between opaque coated panels. The Commission Internationale d'Eclairage (International Commission on Illumination or CIE) lab color system (CIE L*, a*, b*) was used for color measurement. L^*, a^*, and b^* represent three coordinates of the three-dimensional lab color space. These parameters are defined based on the high and low values they represent to identify colors as described as follows:

- L* = 0 represents black, while L^* = 100 represents diffuse white.
- Positive values of a* indicate green, while negative values indicate magenta.
- Positive values of b* indicate blue, while negative values indicate yellow.
- The asterisk is used to differentiate the CIE L*, a*, b* system from (L, a, b) parameters of the original Hunter 1948 color space.

Colors were measured for unscribed test panels before and after ALT and outdoor exposure tests. Three color readings were obtained for each type I panel, and six color readings were obtained for each type II panel. Color difference (ΔE) of the test panels before and after the test was calculated using the equation in figure 11.

$$\Delta E = [(\Delta L^*)^2 + (\Delta a^*)^2 + (\Delta b^*)^2]^{1/2}$$

Figure 11. Equation. Measurement of color.

Where:

$\Delta L^* = L^*_{\text{after test}} - L^*_{\text{before test}}$.
$\Delta a^* = a^*_{\text{after test}} - a^*_{\text{before test}}$.
$\Delta b^* = b^*_{\text{after test}} - b^*_{\text{before test}}$.

The data used in the above equation were the mean of the data obtained from all the unscribed test panels of each coating system.

Adhesion Strength

The adhesion strength of the coating systems was determined using two commercially available pull-off adhesion testers following ASTM D4541-09e1, "Standard Test Method for Pull-Off Strength of Coatings Using Portable Adhesion Testers."[17] A loading fixture, commonly known as a dolly or stub, is affixed to the panel surface by an adhesive. A load provided by the adhesion tester is increasingly applied to the dolly until it is pulled off. The force required to pull the dolly off yields the tensile strength in pounds per square inch (psi). Failure will occur along the weakest plane(s) within the testing system comprised of the dolly, adhesive, individual layers of the coating system, and substrate.

The surface of coated test panels and the base of the dollies were cleaned with detergent water and were lightly roughened with an abrasive pad. The dollies were glued on the test panel surface using a high-strength epoxy adhesive. The cut through the coating around the edge of the dolly was made using a drill press after the complete curing of the adhesive, as seen in figure 12. The initial and final adhesion strengths of coating systems were measured by hydraulic method. Figure 13 shows the hydraulic adhesion tester used in this study. For each coating system, three pull-off adhesion tests were performed on two unscribed virgin type I panels and on each of the tested type I panels. No adhesion strength tests were performed on type II panels.

Figure 12. Photo. Drill press to score a test area around a dolly.

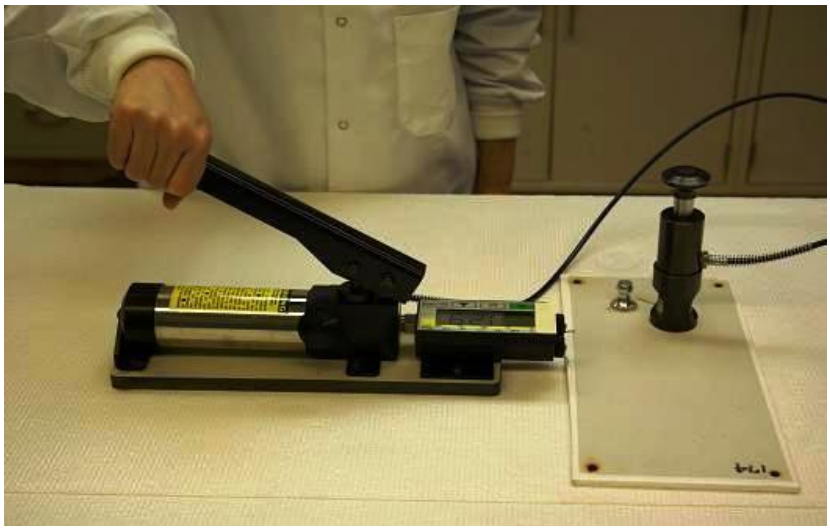

Figure 13. Photo. Hydraulic adhesion tester.

For every panel, the average adhesion strength of three locations was calculated. If the coefficient of variance (CV) of each test panel was more than 20 percent, the test panel and adhesion failure mode were carefully examined to see if the variation was caused by test operation. Repeated tests were performed for quality assurance. If more than 50 percent of a glue failure occurred, the test was also repeated. The reported adhesion strength for each coating system was the mean of the data obtained from tests conducted on all test panels of the coating system. The remaining DFT at the pull-off spots was measured and recorded. The adhesion failure mode of every spot was also documented using digital photographs.

Detection of Coating Defects

The coating defects were identified according to ASTM G62-07, "Standard Test Methods for Holiday Detection in Pipeline Coatings (Method A)."[18] This technique utilizes a low voltage holiday detector to determine the presence of electrically conductive coating defects including holidays (invisible defects with naked eyes) and pinholes, voids, mechanical coating damage, or metal particles protruding through the coating. The reported number of defects after each test cycle was the cumulative number of defects. In addition to using the holiday detector, test panels were visually examined for blisters and rust spots per ASTM D714-02, "Standard Test Method for Evaluating Degree of Blistering of Paints" and ASTM D610-01, "Standard Test Method for Evaluating Degree of Rusting on Painted Steel Surfaces."[19,20] The reference standards were employed to grade the rust pits and surface blisters on the panels.

Rust Creepage Measurement

The rust creepage at the scribe was measured following ASTM D7087-05a, "Standard Test Method for An Imaging Technique to Measure Rust Creepage at Scribe on Coated Test Panels Subjected to Corrosive Environments."[21] The rust creepage area from the scribe line on the coating panel was traced using a thin marker and a transparent plastic sheet. The tracing image was scanned and analyzed using imaging software to obtain the creepage areas and the creepage distances. Two traces for each test panel were obtained, and the mean creepage distance was reported as the nominal creepage at the time of measurement for the coating system.

Digital Microscopic Examination

When unusual surface failures were detected by the holiday detector, such panels were examined using a stereomicroscope or a high-power digital microscope. The surface conditions were documented via microphotographs.

Digital Photography

Every test panel was photographed to document surface conditions before initiating the tests as well as after each test cycle for both ALT and outdoor exposure tests.

EIS

The impedance of the coating systems was measured by EIS using an electrochemical instrument equipped with a potentiostat. This technique involves applying a small amplitude alternating current signal into a body of material over a wide range of frequencies and measuring the responding current and its phase angle shift. The output from the EIS instrument is an impedance spectrum of the material, typically ranging from 100 kHz to 0.001 Hz. EIS data are analyzed by the equivalent circuit modeling technique, which can produce appropriate models to evaluate the coating deterioration process and the mechanism of corrosion occurring at the interface between the substrate and the coating. Analysis of the EIS data is not included in this report, and the analysis results will be presented in a separate report in the future.

CHAPTER 3. TEST RESULTS AND DISSCUSION

Initial coating characterization results and test results from ALT and outdoor exposure tests pertaining to color, gloss, DFT, pull-off adhesion, surface appearance, surface defects, and rust creepage are presented in this chapter with some supplementary digital images.

3.1 INITIAL CHARACTERIZATION OF COATING SYSTEMS

DFT

Table 5 and figure 14 show mean DFT, standard deviation, and CV of the coating systems measured on type I panels. DFT varied significantly from 7.5 to 17.8 mil depending on the coating system.

Table 5. DFT data for type I panels.

Coating System	Number of Coats	Mean (mil)	Standard Deviation (mil)	CV (Percent)
IOZ/E/PU	3	13.03	0.66	5.07
ZE/E/PU	3	14.31	0.84	5.87
MCU/E/F	3	13.31	0.67	5.03
ZE/PU	2	7.75	0.56	7.23
Zn/PS	2	7.5	0.46	6.13
TSZ/LE	2	15.97	1.31	8.2
ZnE/LE	2	17.87	1.26	7.05
HRCSA	1	8.3	0.53	6.39

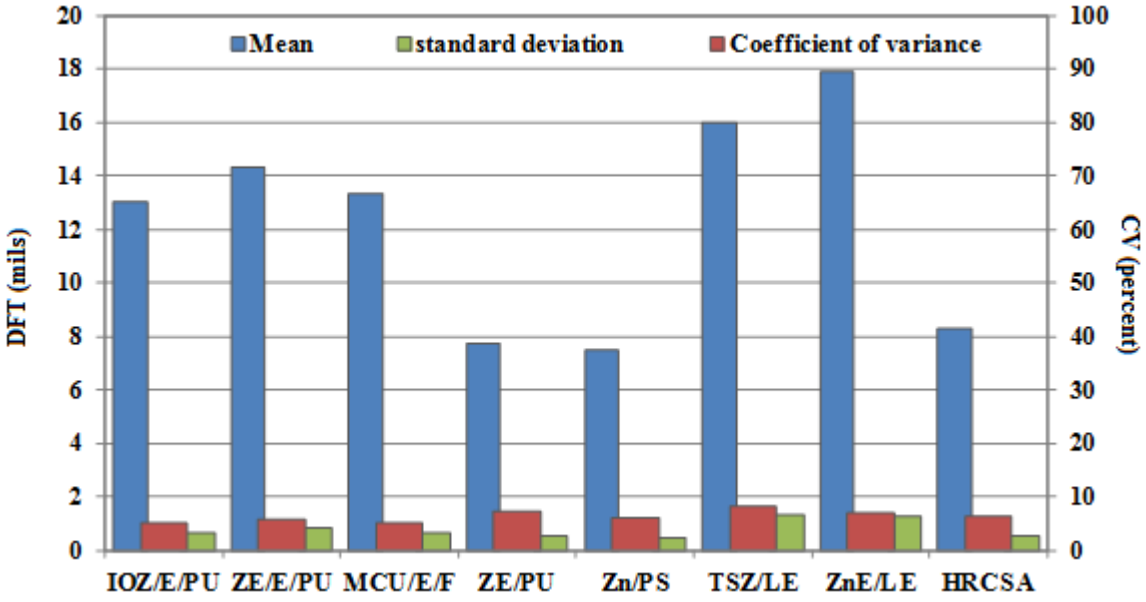

Figure 14. Graph. DFT data (type I panels).

None of the mean DFTs was less than 7 mil, and two of the two-coat systems (ZE/PU and Zn/PS) were between 7 and 8 mil. All three-coat systems (IOZ/E/PU, ZE/E/PU, and MCU/E/F) had mean DFTs between 13 and 15 mil. The remaining two-coat systems (TSZ/LE and ZnE/LE) had the highest DFT values (16–18 mil) and the largest variation of DFT data in terms of CV and standard deviation. The one-coat system (HRCSA) had a DFT of 8.3 mil, which was slightly thicker than two of two-coat systems, ZE/PU and Zn/PS.

Gloss

Figure 15 shows the initial mean gloss readings of type I and type II panels. The eight coating systems exhibited a wide range of initial gloss, with HRCSA having the lowest gloss reading of 9.5 and MCU/E/F, Zn/PS, TSZ/LE, and ZnE/LE having the high gloss readings greater than 70. The other coating systems, IOZ/E/PU, ZE/E/PU, and ZE/PU, possessed intermediate gloss. In most cases, the coating systems exhibited different gloss readings depending on the type of panel (i.e., type I versus type II). This observation suggests that absolute gloss readings may not be useful due to inherent variation of the measurement technique.

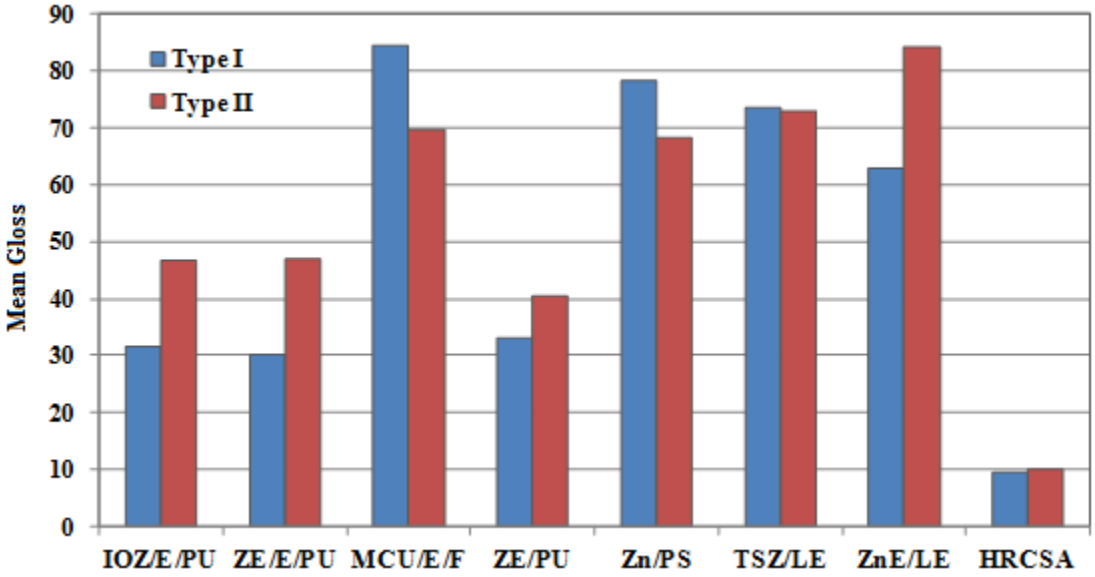

Figure 15. Graph. Initial mean gloss.

Color

Initial mean color readings are summarized in table 6. To calculate change of color (ΔE), color readings made at different times were necessary, as shown in the equation in figure 11.

Table 6. Initial mean color readings.

Coating System	Number of Coats	Type 1			Type II		
		L*	a*	b*	L*	a*	b*
IOZ/E/PU	3	68.83	-1.64	6.20	68.70	-1.68	6.47
ZE/E/PU	3	68.84	-1.64	6.18	68.82	-1.58	6.46
MCU/E/F	3	92.66	-0.79	1.23	92.23	-0.84	1.50
ZE/PU	2	68.86	-1.64	6.13	68.72	-1.67	6.46
Zn/PS	2	96.55	-1.35	4.15	94.20	-1.40	3.88
TSZ/LE	2	47.56	-2.72	-0.64	47.08	-2.82	0.46
ZnE/LE	2	48.1	-2.80	-0.26	47.10	-2.81	0.16
HRCSA	1	61.49	-0.69	1.71	61.30	-0.75	1.84

Adhesion Strength

Initial mean adhesion values are shown in table 7 and figure 16. Two of the two-coat systems (ZnE/LE and TSZ/LE) exhibited the highest baseline adhesion strengths of 2,110 and 1,834 psi (CV = 21 and 13 percent), respectively, while the one-coat system (HRCSA) demonstrated the lowest adhesion strength of 259 psi (CV = 45 percent). The poor adhesion strength of HRCSA was observed in a previous FHWA study.[22] The two control coating systems (IOZ/E/PU and ZE/E/PU) had the second and third lowest adhesion strengths of 1,119 and 1,173 psi (CV = 36 and 30 percent), respectively. All remaining three-coat and two-coat systems showed moderate adhesion strengths between 1,200 and 1,400 psi (CV = 17 to 26 percent).

Table 7. Initial pull-off adhesion strength of type I panels.

Coating System	Number of Coats	Average Adhesion Strength (psi)	CV (Percent)	Standard Deviation (psi)
IOZ/E/PU	3	1,119	36	400
ZE/E/PU	3	1,173	30	354
MCU/E/F	3	1,371	26	356
ZE/PU	2	1,314	19	250
Zn/PS	2	1,259	17	213
TSZ/LE	2	1,834	13	242
ZnE/LE	2	2,110	21	433
HRCSA	1	259	45	115

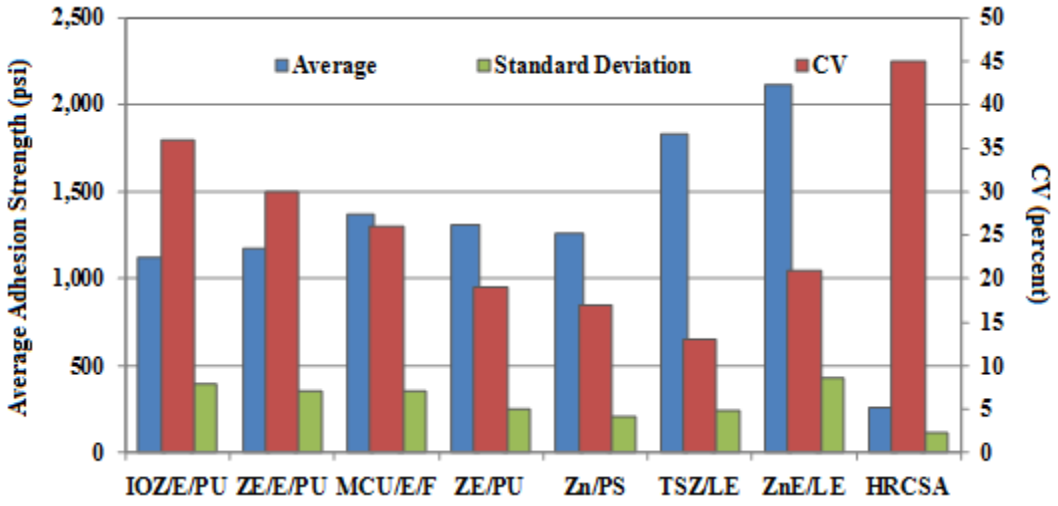

Figure 16. Graph. Initial pull-off adhesion strength data (type I panels).

3.2 PERFORMANCE DURING ALT AND OUTDOOR EXPOSURE TESTING

Performance of the coating systems in ALT, NW, NWS, and GGB was evaluated by the following parameters:

- Gloss reduction.
- Change of color.
- Change of adhesion strength.
- Development of surface defects.
- Growth of rust creepage at the scribe.

Due to premature coating failures of two of the two-coat systems (TSZ/LE and ZnE/LE) in ALT, the study was terminated after 10 cycles of ALT (3,600 h), 10 months of NW and NWS, and 6 months of GGB exposure. Unexpected early termination of the study led to no data collection from type II panels used for 6 months at GGB. Therefore, most outdoor performance is discussed with the NW and NWS data only.

Gloss Reduction

At the termination of the study, gloss data of each coating system were obtained from type I and type II panels exposed to ALT, NW, and NWS environments. Then, gloss reductions of the coating systems after 3,600 h of ALT and 10 months of NW and NWS testing were calculated with respect to their initial readings. Table 8 and figure 17 present the gloss reduction data. The largest gloss reduction was exhibited by two two-coat systems (TSZ/LE and ZnE/LE) and the one-coat system, HRCSA, as shown in figure 17. These coating systems experienced the most dramatic changes from the highest initial gloss readings (two-coat systems) and the lowest gloss reading (one-coat system). It should be noted that the two-coat systems failed prematurely, and

both had the same linear epoxy top coat. Conversely, two other coating systems (MCU/E/F and Zn/PS), which also exhibited high initial gloss readings (see figure 15), exhibited the least amount of changes after testing. The three-coat controls (IOZ/E/PU and ZE/E/PU) and the two-coat system ZE/PU exhibited intermediate initial gloss readings and remained at less than 30 percent gloss reduction after tests. The type II panels in NW tended to show the largest gloss reduction among coating systems, with little to moderate overall gloss reductions.

Table 8. Mean gloss reduction (percent).

Coating System	Number of Coats	Type 1			Type II		
		ALT	NW	NWS	NW	NWS	GGB
IOZ/E/PU	3	12.96	9.47	27.6	27.96	15.15	No data available
ZE/E/PU	3	17.76	14.51	8.89	44.93	20.87	
MCU/E/F	3	0.82	3.65	2.13	30.4	3.17	
ZE/PU	2	14.7	10.07	9.83	24.62	22.28	
Zn/PS	2	-6.88	1.42	-1.61	10.1	3.3	
TSZ/LE	2	94.73	92.63	92.47	95.54	94.97	
ZnE/LE	2	75.6	92.57	96.2	95.39	96.39	
HRCSA	1	24.41	66.9	50.57	68.91	74.81	

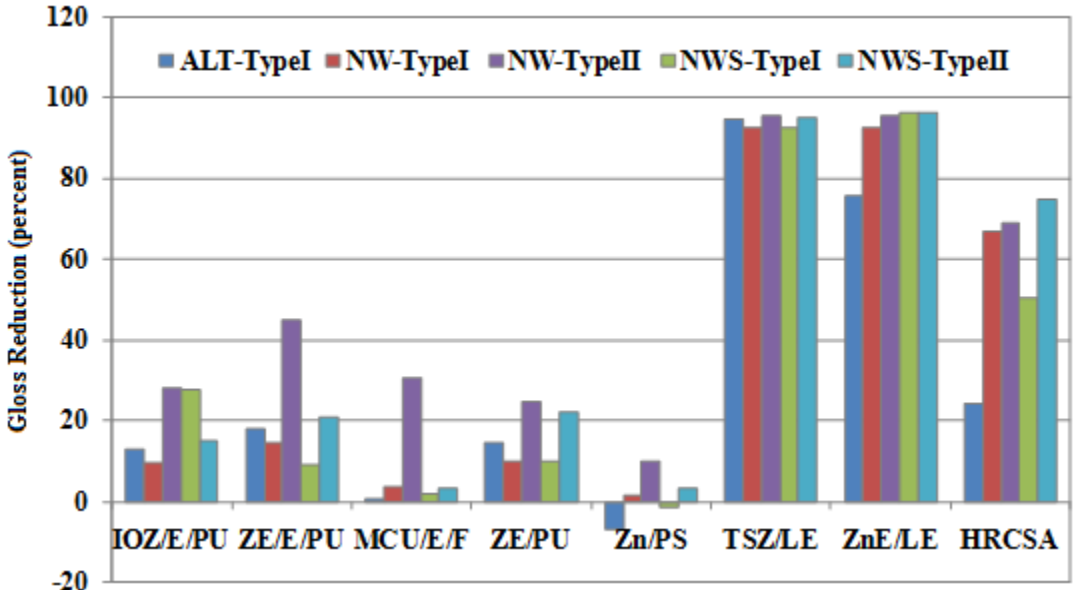

Figure 17. Graph. Mean gloss reduction.

Color Changes

Table 9 and figure 18 show mean color change data. HRCSA exhibited the largest color change, followed by two two-coat systems (TSZ/LE and ZnE/LE). These coating systems exhibited the largest gloss reductions. The others exhibited less than 2 percent color changes after testing. Because of scattered data among different test conditions, effects of salt spray and type of test panel on color change were inconclusive, except that most coating systems exhibited the least amount of color changes in ALT.

Table 9. Mean color changes (percent).

Coating System	Number of Coats	Type 1			Type II	
		ALT	NW	NWS	NW	NWS
IOZ/E/PU	3	0.08	1.34	0.60	0.67	6.43
ZE/E/PU	3	0.32	1.03	0.46	0.63	0.40
MCU/E/F	3	0.12	1.07	0.44	0.27	1.01
ZE/PU	2	0.16	1.16	0.37	0.35	0.71
Zn/PS	2	1.29	0.71	1.25	1.40	0.93
TSZ/LE	2	3.93	3.34	4.60	4.35	3.52
ZnE/LE	2	2.91	2.64	4.04	4.24	3.10
HRCSA	1	2.66	5.14	7.15	7.37	11.96

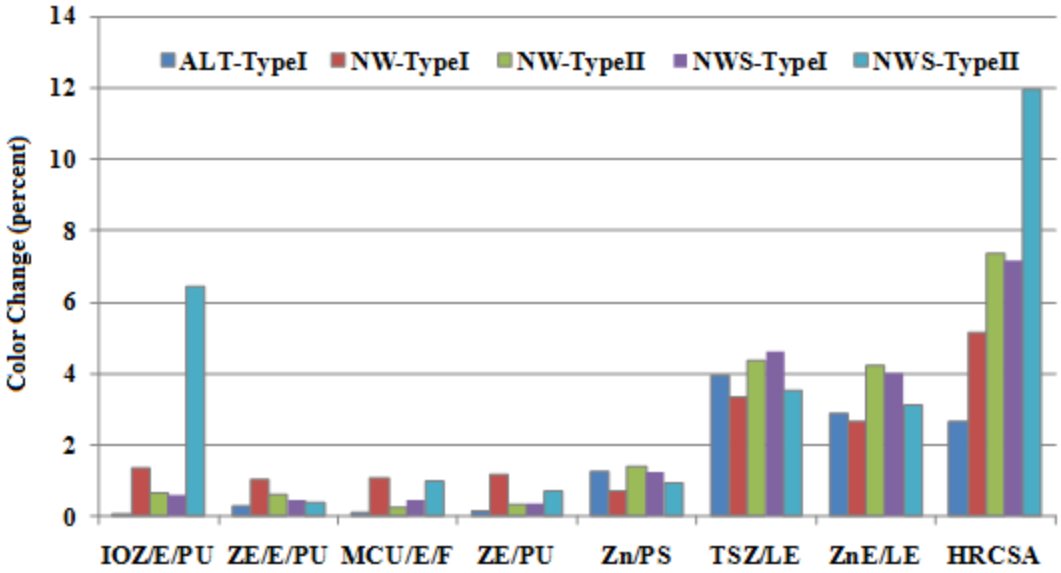

Figure 18. Graph. Mean color changes.

Changes in Adhesion Strength

Adhesion strength changes in type I panels after exposure in ALT, NW, and NWS are summarized in table 10, and the corresponding bar graph is shown in figure 19. All coating systems, except HRCSA and MCU/E/F, showed varying degrees of adhesion strength reduction at the end of testing in every test condition. No clear trend was observed between reduction of adhesion strength and test conditions. It is unclear at this time why HRCSA, which exhibited the weakest initial adhesion strength, had the largest strength gain during testing. However, it may be reasoned that because HRCSA had the weakest coating before and after testing, relatively small increases in post-test absolute adhesion strength resulted in significant increases in terms of percentage. Such a trend was more pronounced for NW and NWS panels than ALT panels. Adhesion strength data for TSZ/LE could not be obtained at the termination of ALT because the coating surface was so blistered that the adhesion dollies did not stick to the surface of the panels. Because ZnE/LE panels had peeling top coats at the end of testing, dollies were carefully placed in areas with intact top coats. ZnE/LE panels had the largest adhesion strength reduction. The two worst performing two-coat systems (TSZ/LE and ZnE/LE) in gloss and color also

suffered from the largest adhesion reductions. The least amount of adhesion strength reduction was seen in both controls (IOZ/E/PU and ZE/E/PU) as well as ZE/PU. The other two-coat system, Zn/PS, had a moderate adhesion strength loss.

Table 10. Mean adhesion strength changes of type I panels.

Coating System	Number of Coats	Initial Adhesion Strength (psi)	Final Adhesion Strength in Exposure Condition (psi)			Percent Change		
			ALT	NW	NWS	ALT	NW	NWS
IOZ/E/PU	3	1,119	818	1,073	1,108	-27	-4	-1
ZE/E/PU	3	1,173	1,135	1,124	1,365	-3	-4	-16
MCU/E/F	3	1,371	1,423	1,561	1,618	4	14	18
ZE/PU	2	1,314	1,176	1,295	1,258	-10	-1	-4
Zn/PS	2	1,259	976	1,036	1,024	-22	-18	-19
TSZ/LE	2	1,834		1,150	911		-37	-50
ZnE/LE	2	2,110	651	1,321	1,207	-69	-37	-43
HRCSA	1	259	312	461	506	21	78	96

Note: Blank cells indicate that final adhesion strength and percent change could not be obtained for TSZ/LE at the termination of ALT.

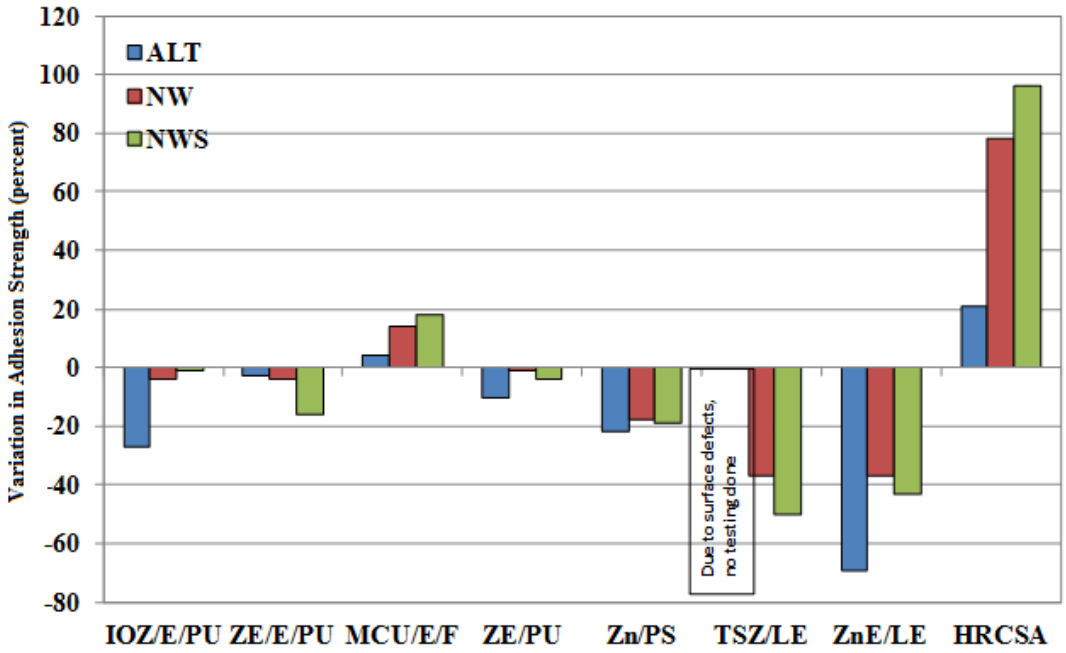

Figure 19. Graph. Mean adhesion strength changes of type I panels.

Development of Surface Defects

ALT

The total number of cumulative surface defects that developed during ALT is listed in table 11, and the corresponding line-scatter graph is shown in figure 20. The exact number of defects could not be counted when an excessive amount was detected. As a result, an arbitrary number

of 100 was entered in the data sheet. Excessive defects were observed on the surface of two two-coat system (TSZ/LE and ZnE/LE) test panels. Even though initial assessment of these coating systems showed no defects, including invisible defects (holidays), on the surface, a sudden increase in the number of defects during ALT led to severe surface deterioration as indicated by blistering, rusting, and/or cracking, which is discussed in the next section.

In the case of TSZ/LE, one of the panels developed four defects after 1,080 h of testing, and the number of defects increased excessively after 1,440 and 1,800 h of testing. These surface defects were then followed by excessive blistering and cracking of the surface. For ZnE/LE, no defects were detected until 2,880 h of testing. Progressive changes were observed leading to surface microcracks, which transformed to macrocracks. As shown in table 11, MCU/E/F did not develop any defects, while other coating systems only developed minimal coating defects upon termination of ALT at 3,600 h.

Table 11. Cumulative number of surface defects developed during ALT.

Time (hours)	IOZ/E/PU	ZE/E/PU	MCU/E/F	ZE/PU	Zn/PS	TSZ/LE	ZnE/LE	HRCSA
0	0	0	0	0	0	0	0	0
360	0	1	0	0	0	1	0	1
720	0	1	0	0	0	1	0	1
1,080	0	1	0	0	0	4	0	1
1,440	0	1	0	0	1	100	0	1
1,800	0	1	0	1	1	100	0	1
2,160	0	1	0	1	1	100	0	1
2,520	0	1	0	1	1	100	0	1
2,880	2	1	0	1	1	100	2	1
3,240	2	2	0	3	2	100	100	1
3,600	2	2	0	3	2	100	100	1

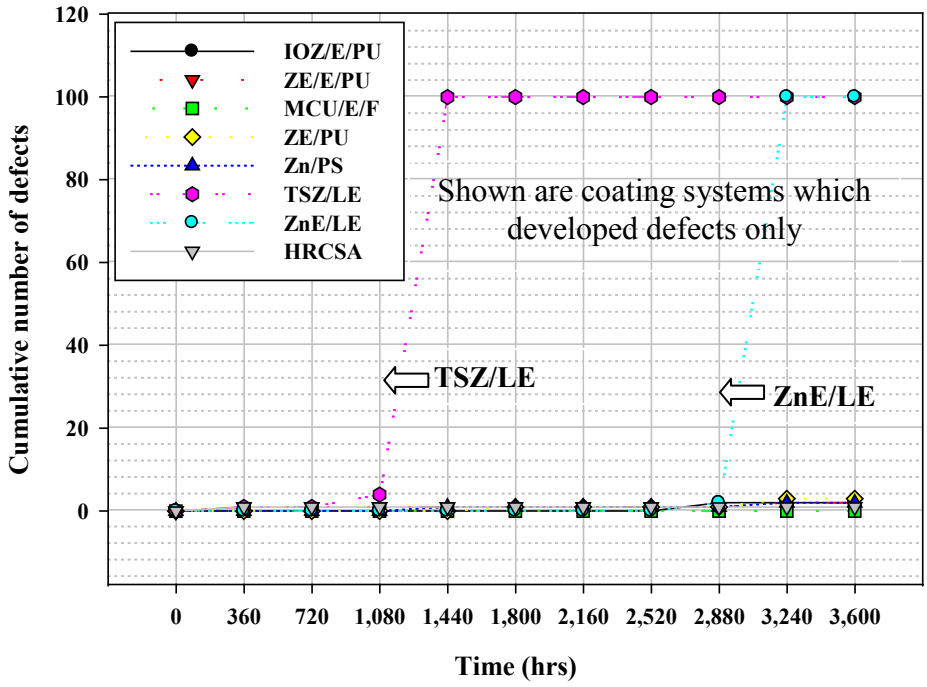

Figure 20. Graph. Cumulative number of surface defects developed on type I panels during ALT.

NW and NWS

Most of the type I panels did not develop any defects during outdoor exposure in NW and NWS. Exceptions were two of the two-coat systems, TSZ/LE and ZnE/LE, which performed poorly in other tests. TSZ/LE exhibited countless defects on every NW and NWS type I panel. For ZnE/LE, five defects on NW panels and seven defects on NWS panels were developed after 10 months of outdoor testing. All type I and type II test panels employed in NW and NWS developed many defects along the panel edges. Type II panels also had coating defects in areas such as nuts, bolts, underside of the T-attachment, and the wide-angle attachment due to less than ideal coating application conditions. As expected, these defects became rust spots. This finding confirms that it is difficult to avoid initial coating defects from coating applications on field bridge structures due to complex shapes of structural elements. These imperfect sites are prone to advanced coating failures and subsequent steel corrosion in service environments.

Table 12 lists coating defect development for type II panels. For the sake of simplicity in this report, only DFT-measured flat areas on all panels were studied for defect development. Zn/PS initially contained numerous coating defects in the low DFT areas, and none of the high and normal DFT areas developed additional defects during outdoor exposure testing. Although TSZ/LE started with a moderate number of coating defects in the low DFT and six in the normal DFT areas, they ended up with numerous defects on every panel regardless of DFT and exposure condition. Also, the low DFT area of the ZnE/LE coating system in NWS developed greater than 70 percent surface deterioration accompanied by surface cracking and coating failure. HRCSA started with 3 initial defects and developed 15 defects in the low DFT and 1 defect in the normal DFT areas in both NW and NWS. The 15 defects in the NW and NWS environments appeared to be related to mechanical damage through the soft coating. The other coating systems did not

develop additional coating defects during the 10 months of exposure testing. Coating defect data were not available for the panels at the GGB exposure site.

Table 12. Number of surface defects developed on type II panels during NW and NWS exposure testing.

Coating System	Exposure	Initial			After 10 months of Exposure Testing		
		L	H	N	L	H	N
IOZ/E/PU	NWS	0	0	0	0	0	0
	NW	0	0	0	0	0	0
ZE/E/PU	NWS	2	0	0	2	0	0
	NW	0	0	0	0	0	0
MCU/E/F	NWS	0	0	0	0	0	0
	NW	0	0	0	0	0	0
ZE/PU	NWS	0	0	0	0	0	0
	NW	0	0	0	0	0	0
Zn/PS	NWS	Numerous defects	0	0	Numerous defects	0	0
	NW	Numerous defects	0	0	Numerous defects	0	0
TSZ/LE	NWS	> 50	0	6	Numerous defects	Numerous defects	Numerous defects
	NW	> 25	0	0	Numerous defects	Numerous defects	Numerous defects
ZnE/LE	NWS	0	0	0	> 70 percent failure	0	0
	NW	0	0	0	0	0	0
HRCSA	NWS	0	0	1	6	0	1
	NW	0	0	2	8	0	3

Rust Creepage

ALT

Table 13 and figure 21 show rust creepage data measured during 3,600 h of ALT. Because all of the TSZ/LE panels started to develop serious surface deterioration after only 1,080 h of ALT, rust creepage data from this coating system were not measured.

Based on the mean creepage values at the end of 3,600 h of ALT, the coating systems were ranked in the following order from highest to lowest rust creepage:

$$\text{MCU/E/F} \gg \text{ZE/E/PU} \approx \text{Zn/PS} \approx \text{ZE/PU} \approx \text{ZnE/LE} > \text{IOZ/E/PU} > \text{HRCSA}$$

It should be noted that ZE/E/PU creepage data showed a steadily decreasing trend during the last three cycles, which was caused by measurement errors. Based on a rapid creepage growth of ZnE/LE observed from the sixth cycle (2,520 h), it can be projected that the coating system

would have shown a very high rust creepage if ALT had continued for more cycles. As observed in previous a FHWA one-coat study, HRCSA had the best performance for resistance to rust creepage.[22]

Table 13. Rust creepage growth during ALT (mm).

Time (hours)	IOZ/E/PU	ZE/E/PU	MCU/E/F	ZE/PU	Zn/PS	ZnE/LE	HRCSA
0	0	0	0	0	0	0	0
360	0	0	0	0.09	0	0	0.18
720	0	0.66	0	0.29	0	0	0.25
1,080	0	0.59	0.82	0.43	0.22	0	0.24
1,440	0	0.88	0.88	0.45	0.37	0	0.25
1,800	0.27	1.15	1.08	0.59	0.49	0	0.29
2,160	0.29	1.42	2.28	0.97	0.60	0	0.29
2,520	0.64	1.25	2.05	0.98	0.93	0.86	0.31
2,880	0.73	1.42	3.14	1.11	1.03	1.02	0.32
3,240	0.74	1.36	3.43	1.23	1.07	1.07	0.32
3,600	0.77	1.30	3.80	1.20	1.24	Panel removed	0.33

1 inch = 25.4 mm

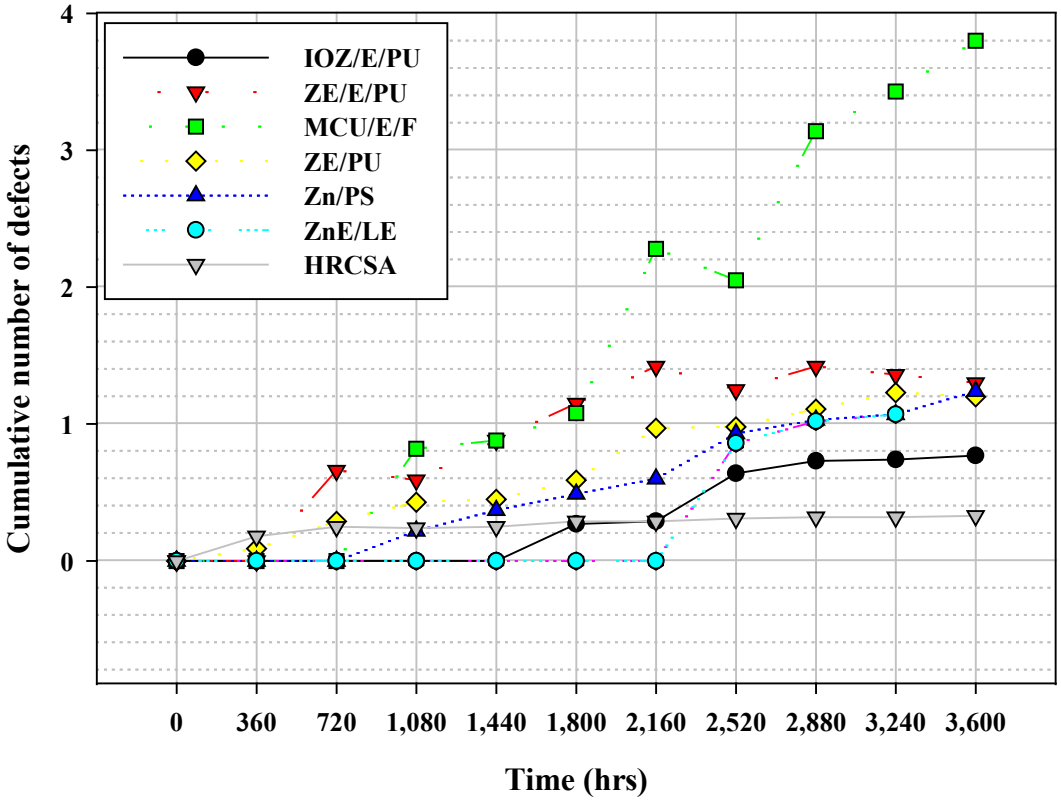

Figure 21. Graph. Rust creepage growth with time during ALT.

NW and NWS

None of the type I panels developed any rust creepage during NW and NWS outdoor exposure testing except for ZnE/LE, which had a rust creepage of 0.16 inches at the end of NWS exposure. After 10 months of exposure of type II panels in NW and NWS testing and 6 months of exposure at the GGB, only the ZnE/LE coating system exhibited recognizable rust creepage, as shown in table 14 and figure 22. High DFT areas of type II panels with ZnE/LE in NWS showed extremely high creepage of around 0.51 inches. Similarly, the nominal DFT area of the same panel showed creepage of about 0.23 inches. The rest of the type II coating systems did not show any rust creepage. It is interesting to observe that ZnE/LE, which was mediocre in ALT, showed the worst rust creepage performance in NW and NWS, whereas MCU/E/F, which performed the worst in ALT, performed well in NW and NWS without rust creepage.

Table 14. Rust creepage growth of ZnE/LE during outdoor exposure.

Coating System	Exposure	DFT Area	Rust Creepage Area (inches^2)
ZnE/LE (type I)	NWS	N	0.52
ZnE/LE (type II)	NW	N	0.30
	NWS	H	1.59
		L	0.46
		N	0.65
	GGB	H	0.30

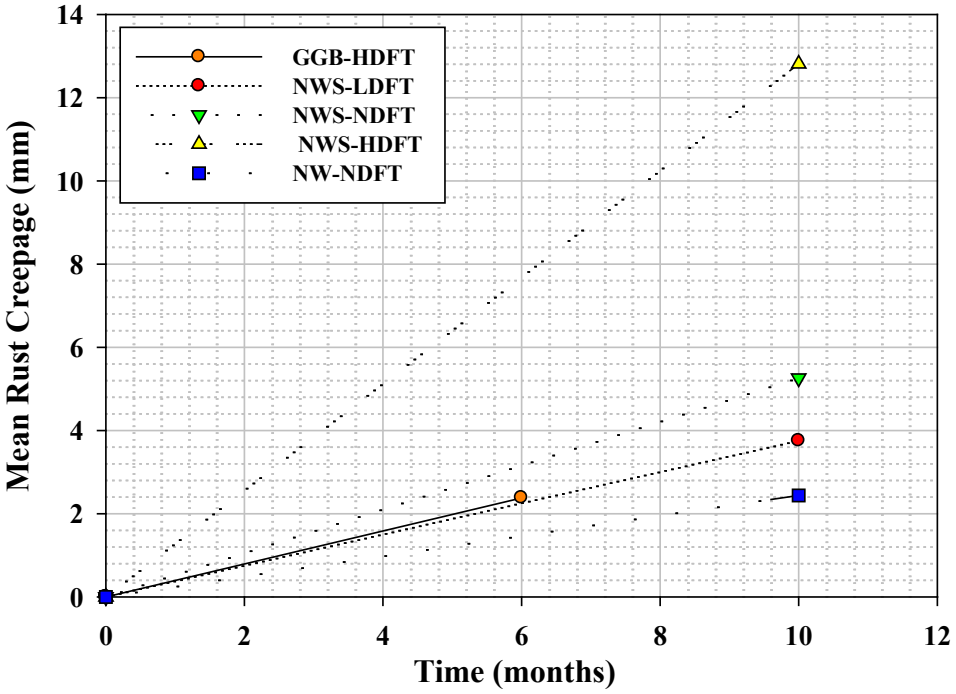

1 inch = 25.4 mm

Figure 22. Graph. Rust creepage growth of ZnE/LE (type II panels).

Physical Condition of Representative Test Panels

Figure 23 through figure 30 show typical digital photographs of all coating systems for type I panels during ALT at 0, 1,440, 2,520, and 3,600 h. These figures also show representative photographs of the type I panels in NW and NWS before and at the termination of testing at 10 months.

ALT

The two controls, IOZ/E/PU and ZE/E/PU (see figure 23 and figure 24), had the best surface retention properties in all exposure conditions despite the fact that ZE/E/PU exhibited the second highest rust creepage. The one-coat system, HRCSA, also retained good surface characteristics with the least rust creepage and minimal defect development despite the fact that it exhibited the third largest gloss reduction and the highest color change (see figure 30). As observed in a previous FHWA one-coat study, HRCSA remained very soft throughout the testing.[22] The third three-coat system, MCU/E/F did not develop defects, but it had the highest creepage at the termination of ALT (see figure 25). Two of the two-coat systems, ZE/PU and Zn/PS, had moderate defect development and rust creepage growth (see figure 26 and figure 27). The remaining two-coat systems, TSZ/LE and ZnE/LE, had the worst surface deterioration over time in ALT as indicated by the development of defects, surface blistering, coating peel-off, and/or surface cracking (see figure 28 and figure 29).

The visual observation of surface changes was followed up with digital microscopy of the test panel surfaces. Digital microscopy of TSZ/LE showed the various phases of progressive deterioration of the coating system at 0, 1,800, and 3,600 h (see figure 31). At 1,800 h, the surface of the coating started to develop blisters, which progressively grew to form a completely blistered coating surface at the termination of ALT, as shown in figure 31. Certain areas still had blisters intact, while some areas had half-peeled or detached coating from the surface. White residual zinc oxide formed on the surface where the coating had peeled off.

Digital microscopy of ZnE/LE during ALT yielded unexpected critical observations. The surface of the coating system showed microcracks all over the surface of a test panel, as shown in figure 32. The central points at which these microcracks originated were a few mils in size, and the cracks themselves were a few hundred mils in size. The microcracks developed into surface macrocracks at the termination of ALT (see figure 32). However, these test panels did not show any surface defects indicated by closed circuit shorting (beeping) during holiday testing, indicating that the cracks did not develop through the coating thickness and might have formed superficially near the surface. Comparison of digital microscopy images before and after exposure indicated that these crack-originating locations were present on the panel surface before testing. However, cracks that propagated from these locations appeared only after ALT. The density of these cracks did not seem to grow as ALT progressed.

NW and NWS

Figure 23 through figure 30 also show type I panels exposed to NW and NWS. In general, their physical conditions appeared to be better than their counterparts in ALT. TSZ/LE exposed to NWS formed distinctive white zinc oxide within the scribe. Additionally, ZnE/LE and HRCSA

under NWS exposure exhibited heavy rust stains in some areas. Interestingly, none of the TSZ/LE and ZnE/LE type I panels, shown in figure 28 and figure 29, respectively, suffered from the same surface deteriorations of blistering (see figure 31) and cracking (see figure 32) observed on their ALT counterparts. Such a finding suggests that either different deterioration mechanisms worked in ALT and NW/NWS or that 10 months in outdoor exposure testing was not sufficient to introduce significant deterioration.

Figure 33 through figure 40 show digital photographs of all coating systems on type II panels before exposure and at 6 months of outdoor exposure testing at GGB. These figures also show conditions of panels before and after exposure in NW and NWS for 10 months. Although each type II panel consisted of low, high, and nominal DFT areas, rust was observed predominantly at hard-to-reach areas where coating was non-uniformly applied and/or where there were coating defects (bare areas). These areas included nuts, bolts, underside of the T-attachment, and the wide-angle attachment. TSZ/LE showed formation of white zinc oxide within the scribe on all DFT areas as well as along the edges of nuts and bolts and underneath the attachments (see figure 38). The ZnE/LE panel exhibited excessive rusting on all DFT areas and along the edges of nuts and bolts and underneath the attachments in NWS (see figure 39). The same panel also showed rust buildup within the V-notch section where salt water could be collected. This form of deterioration reveals that ZnE/LE was particularly venerable to prolonged exposure to salt water. The low DFT area of this coating system developed cracks all over the surface, which was similar to what was observed toward the end of ALT (see figure 32). The two controls did not show any signs of rusting within the three DFT areas (see figure 33 and figure 34). As observed in ALT, the next best performing coating system in comparison to the two three-coat controls was HRCSA, as indicated by negligible rusting and rust creepage (see figure 40).

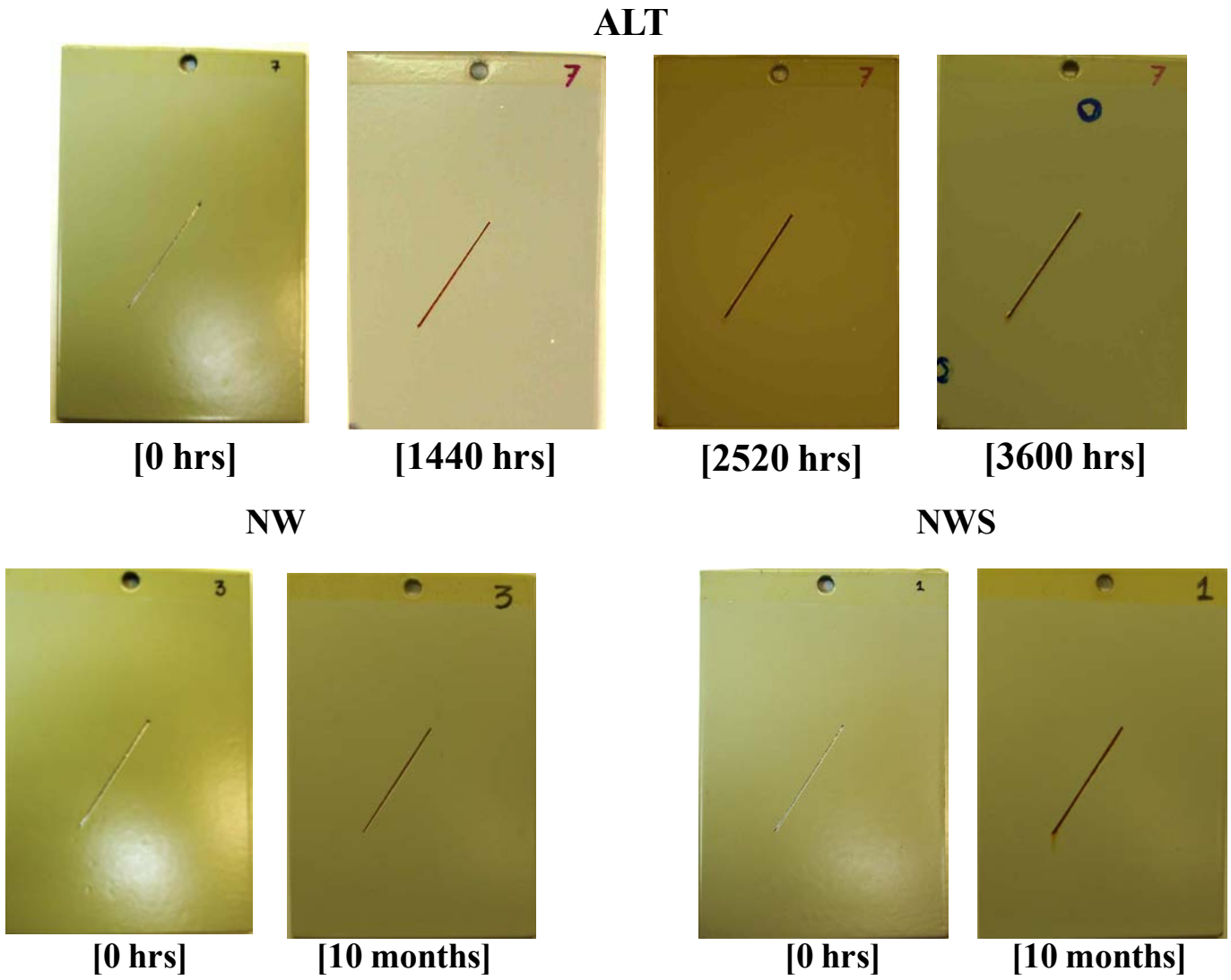

Figure 23. Photo. Progressive changes of IOZ/E/PU—type I in ALT, NW, and NWS.

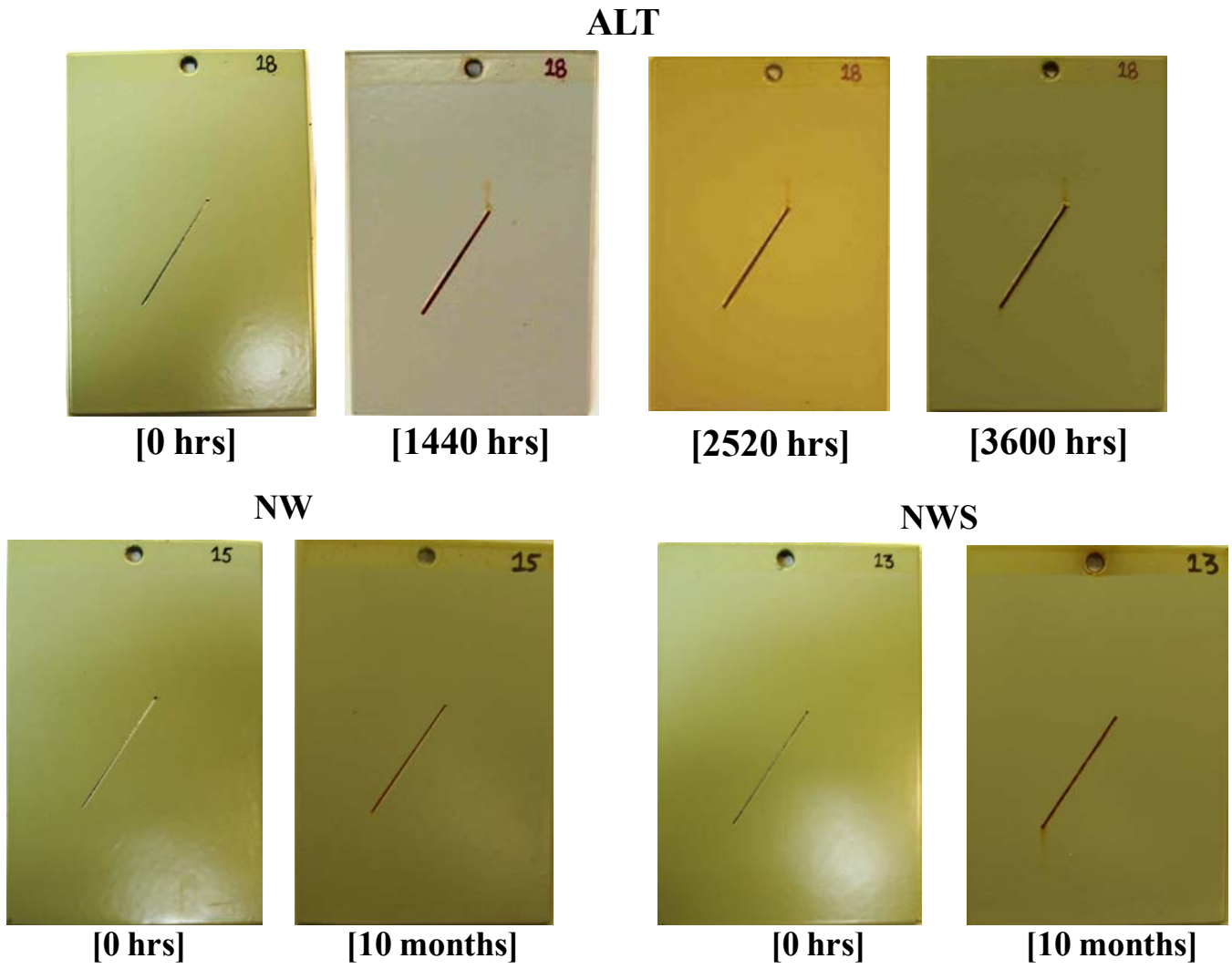

Figure 24. Photo. Progressive changes of ZE/E/PU—type I in ALT, NW, and NWS.

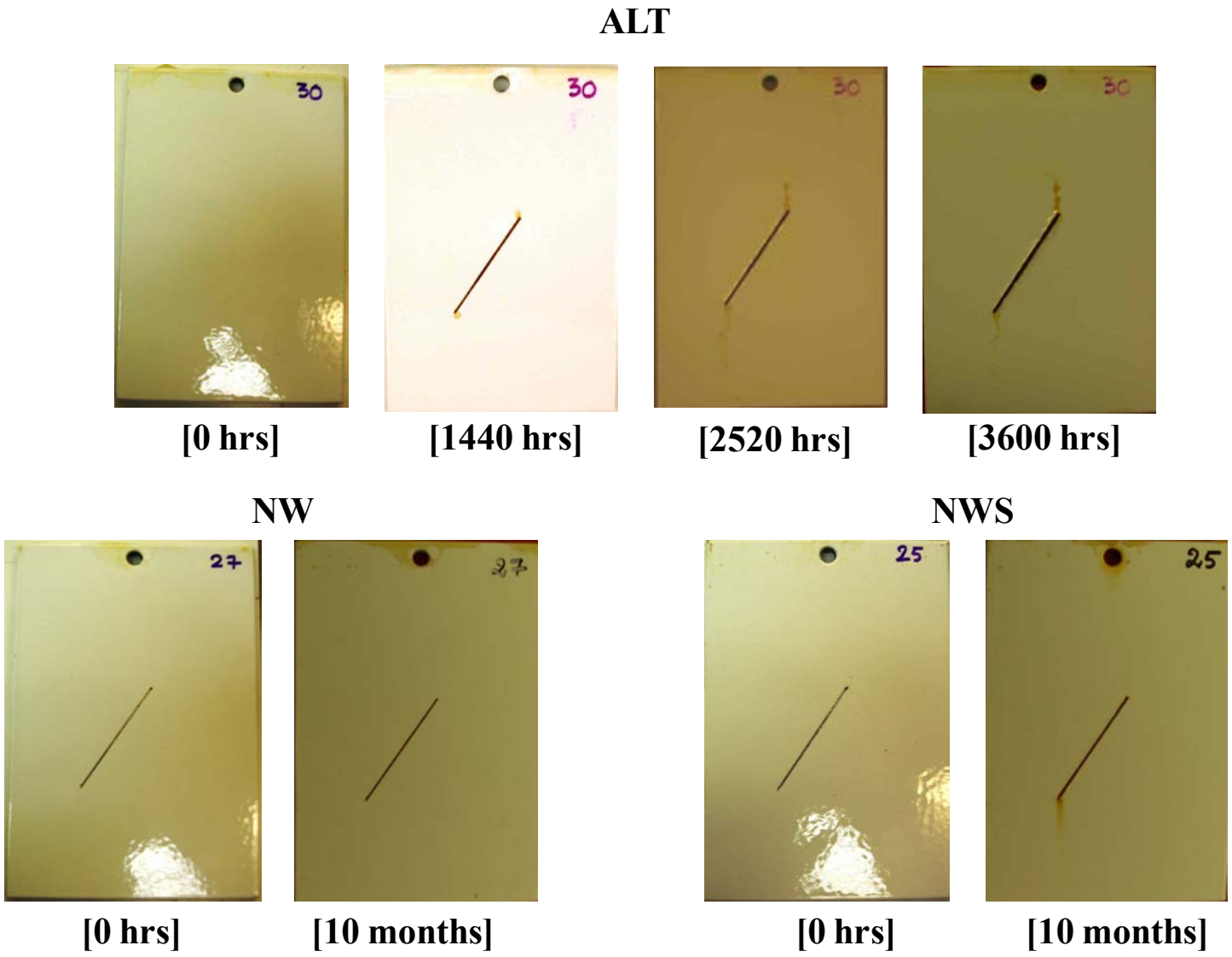

Figure 25. Photo. Progressive changes of MCU/E/F—type I in ALT, NW, and NWS.

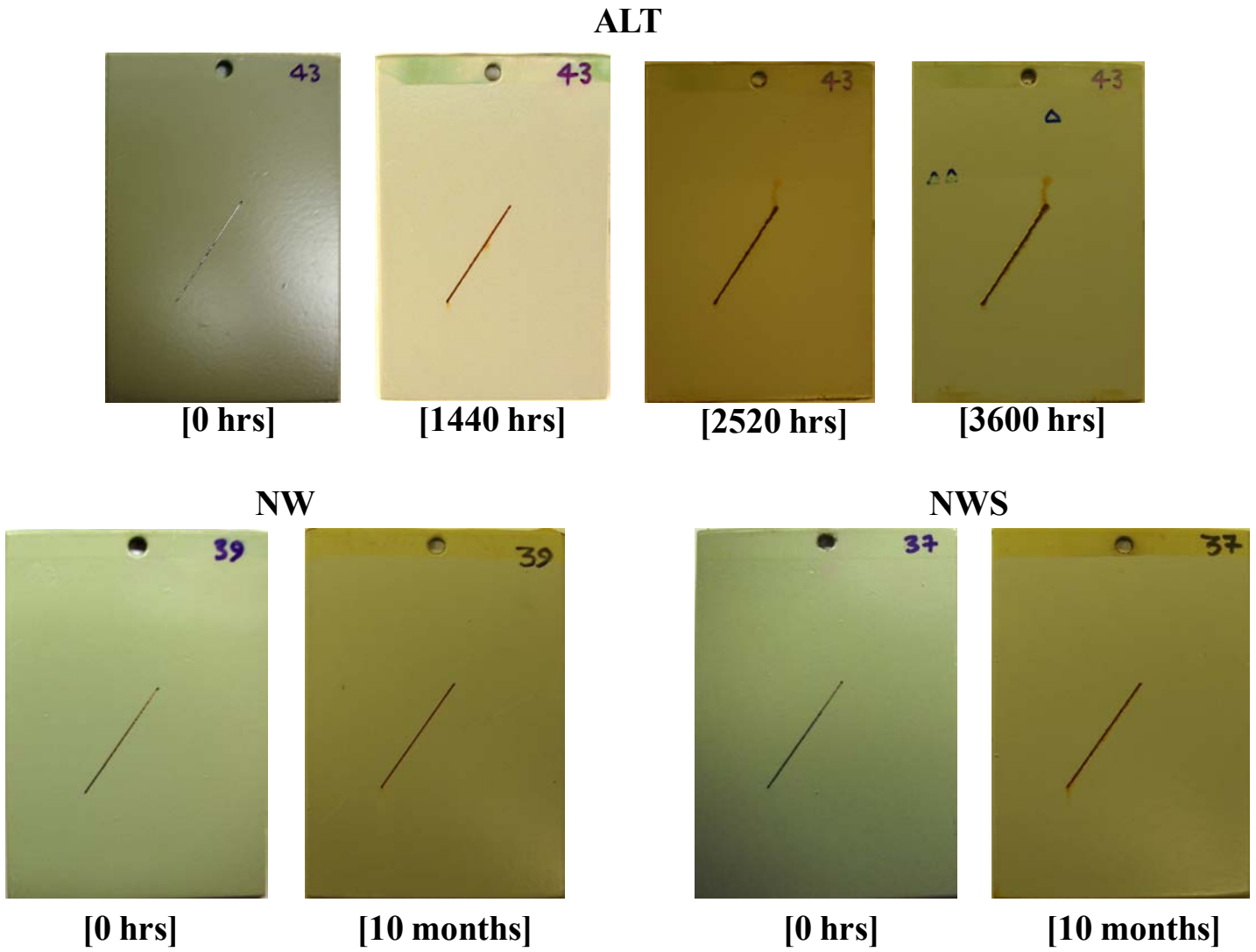

Figure 26. Photo. Progressive changes of ZE/PU—type I in ALT, NW, and NWS.

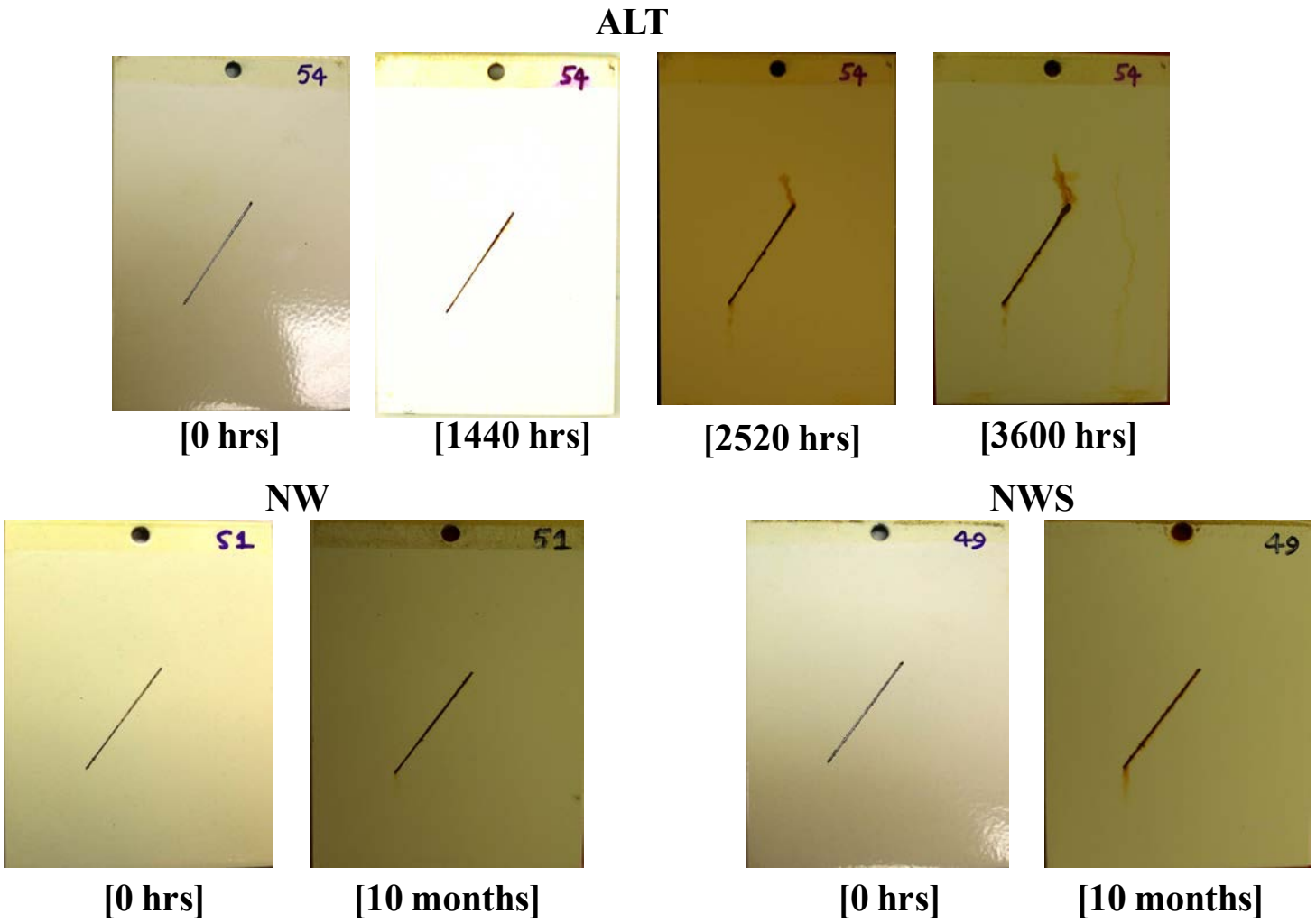

Figure 27. Photo. Progressive changes of Zn/PS—type I in ALT, NW, and NWS.

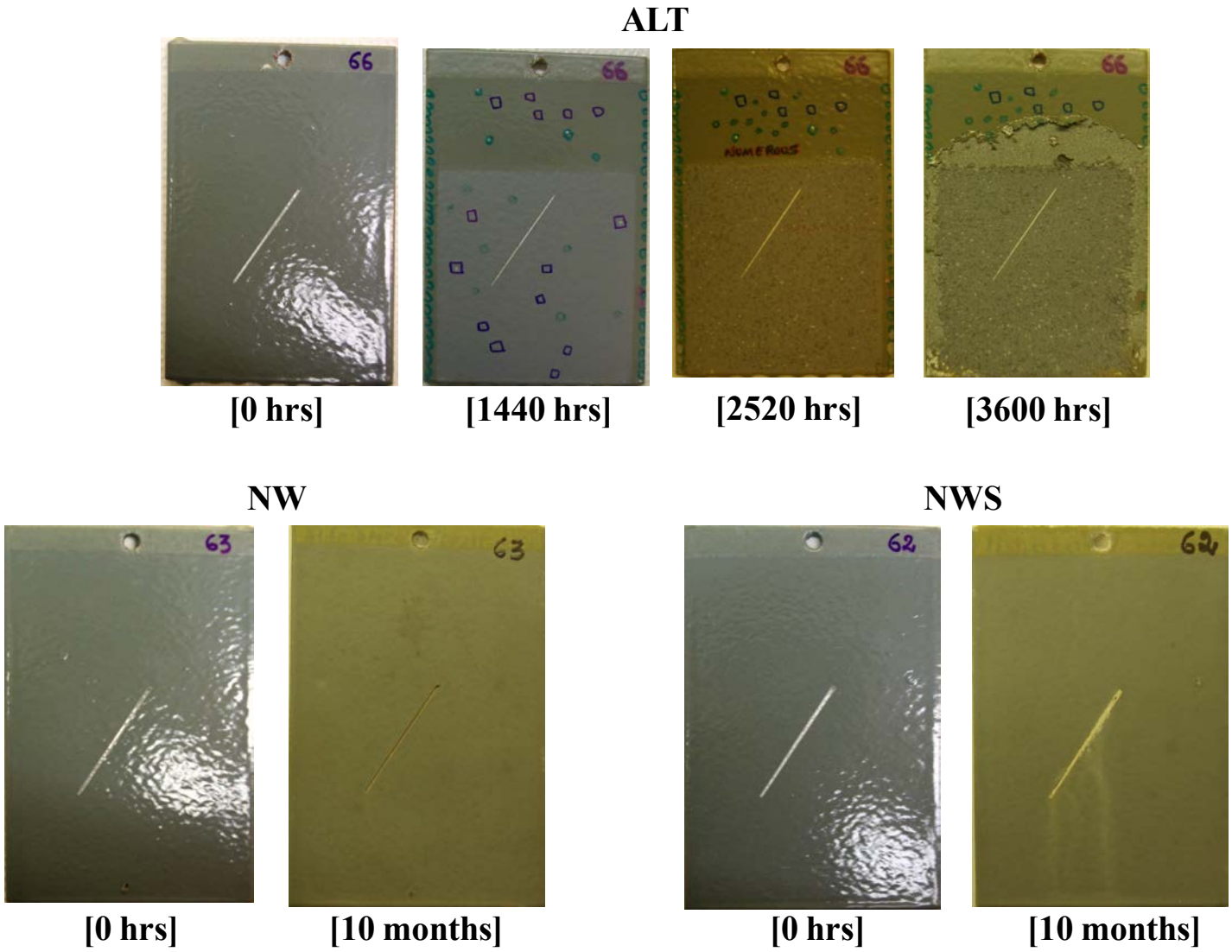

Figure 28. Photo. Progressive changes of TSZ/LE—type I in ALT, NW, and NWS.

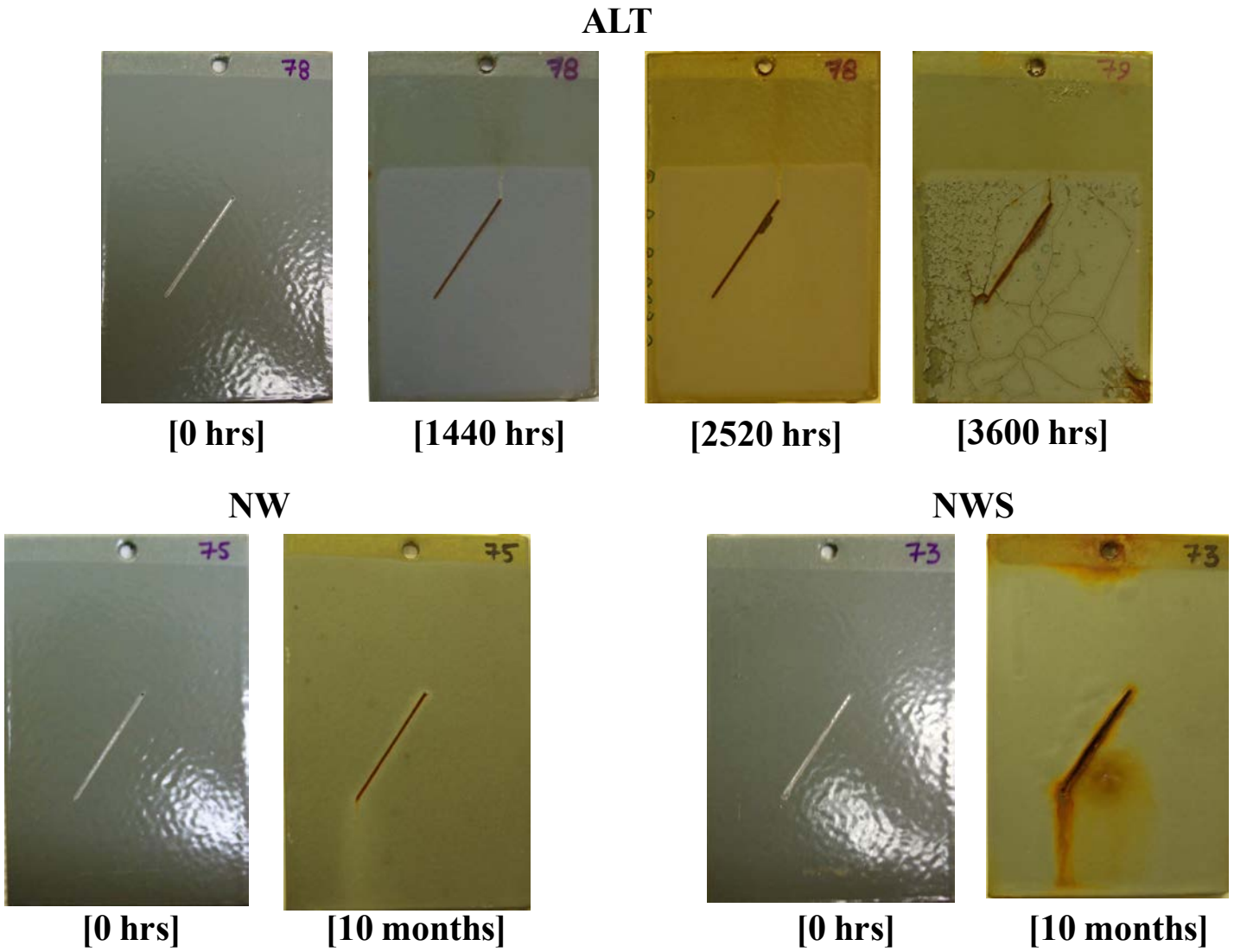

Figure 29. Photo. Progressive changes of ZnE/LE—type I in ALT, NW, and NWS.

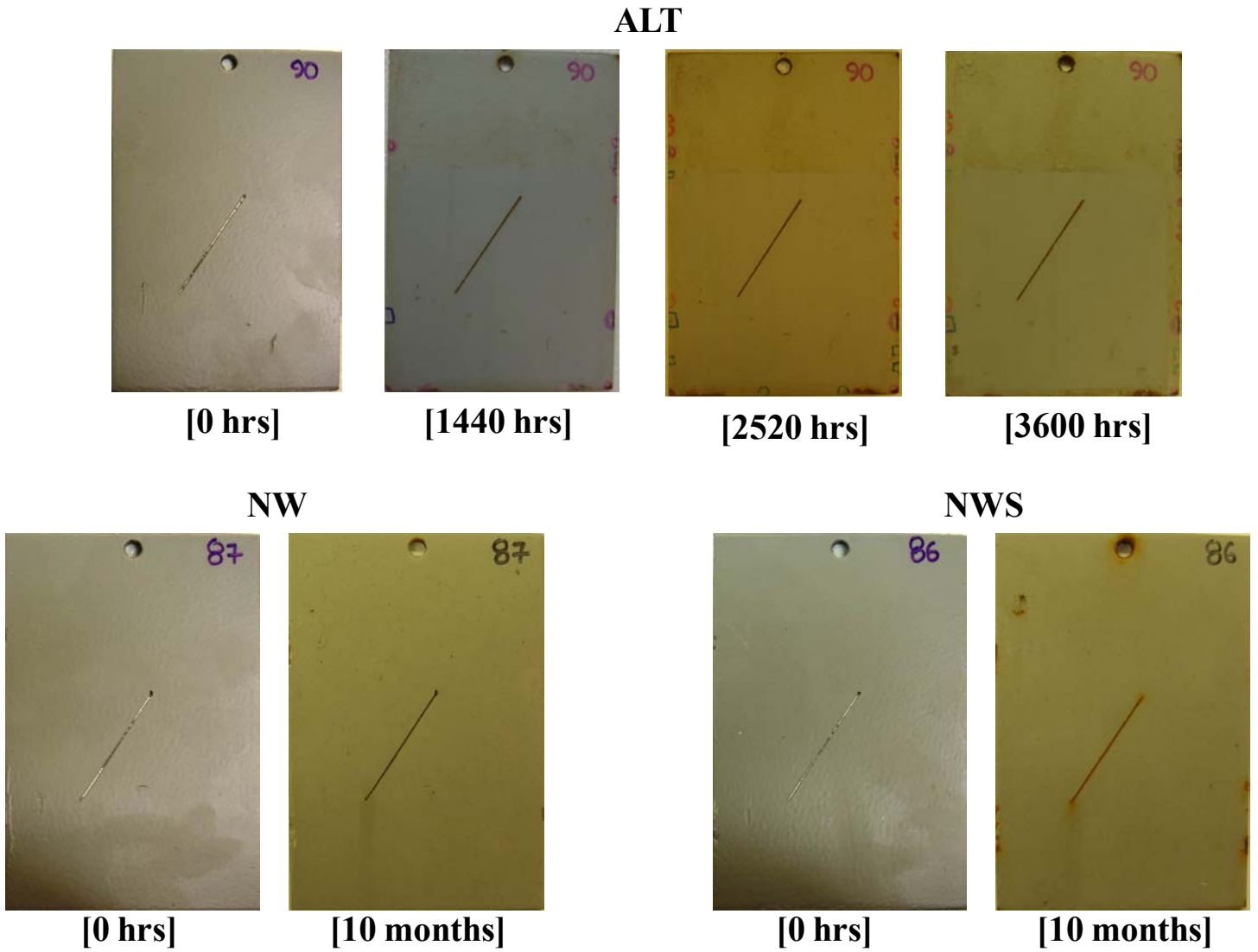

Figure 30. Photo. Progressive changes of HRCSA—type I in ALT, NW, and NWS.

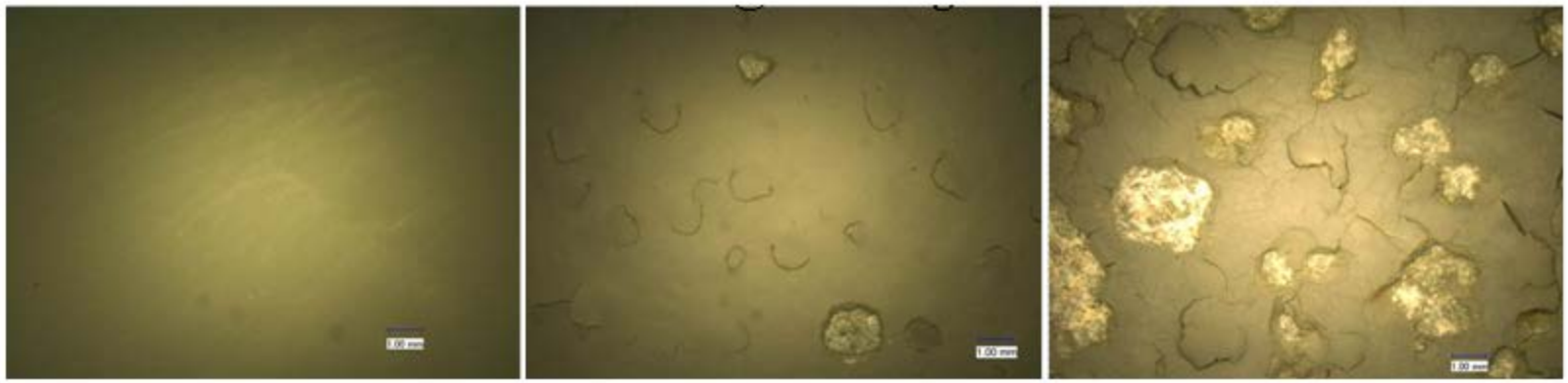

[0 hrs] [1800 hrs] [3600 hrs]

Figure 31. Photo. Photomicrographs of progressive changes of TSZ/LE—type I in ALT.

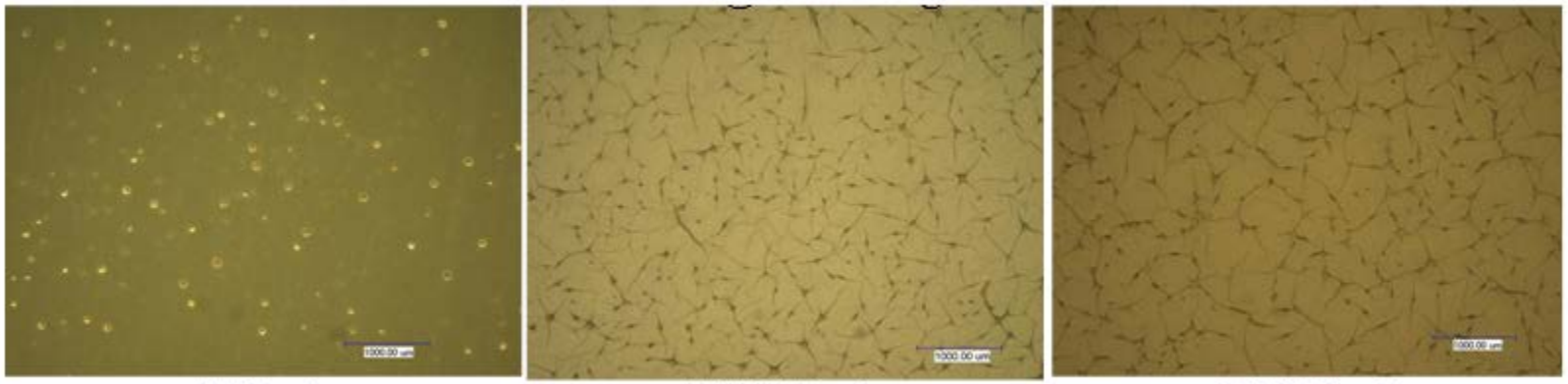

[0 hrs] [1800 hrs] [3600 hrs]

Figure 32. Photo. Photomicrographs of progressive changes of ZnE/LE—type I in ALT.

NW

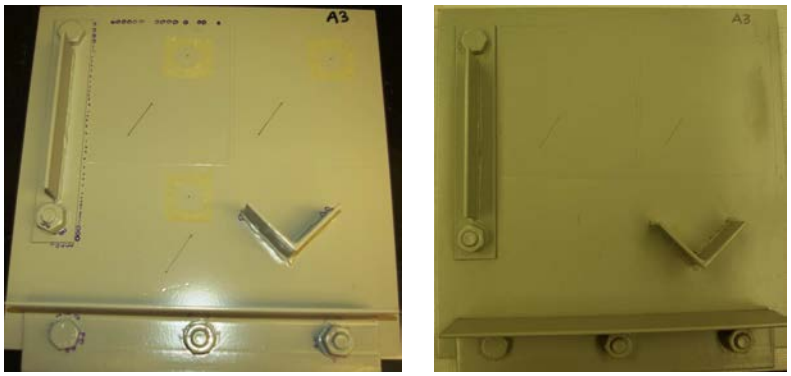

[0 hrs] **[10 months]**

NWS

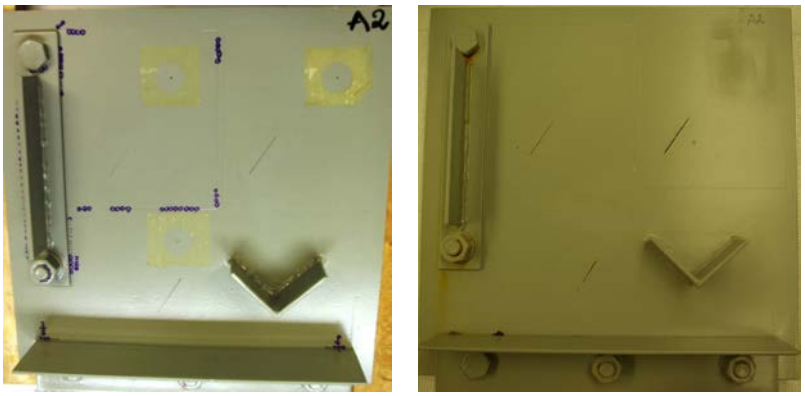

[0 hrs] **[10 months]**

GGB

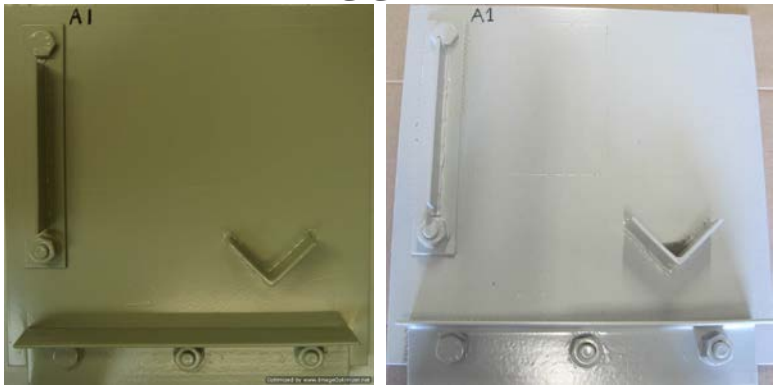

[0 hrs] **[6 months]**

Figure 33. Photo. Progressive changes of IOZ/E/PU—type II in NW, NWS, and GGB.

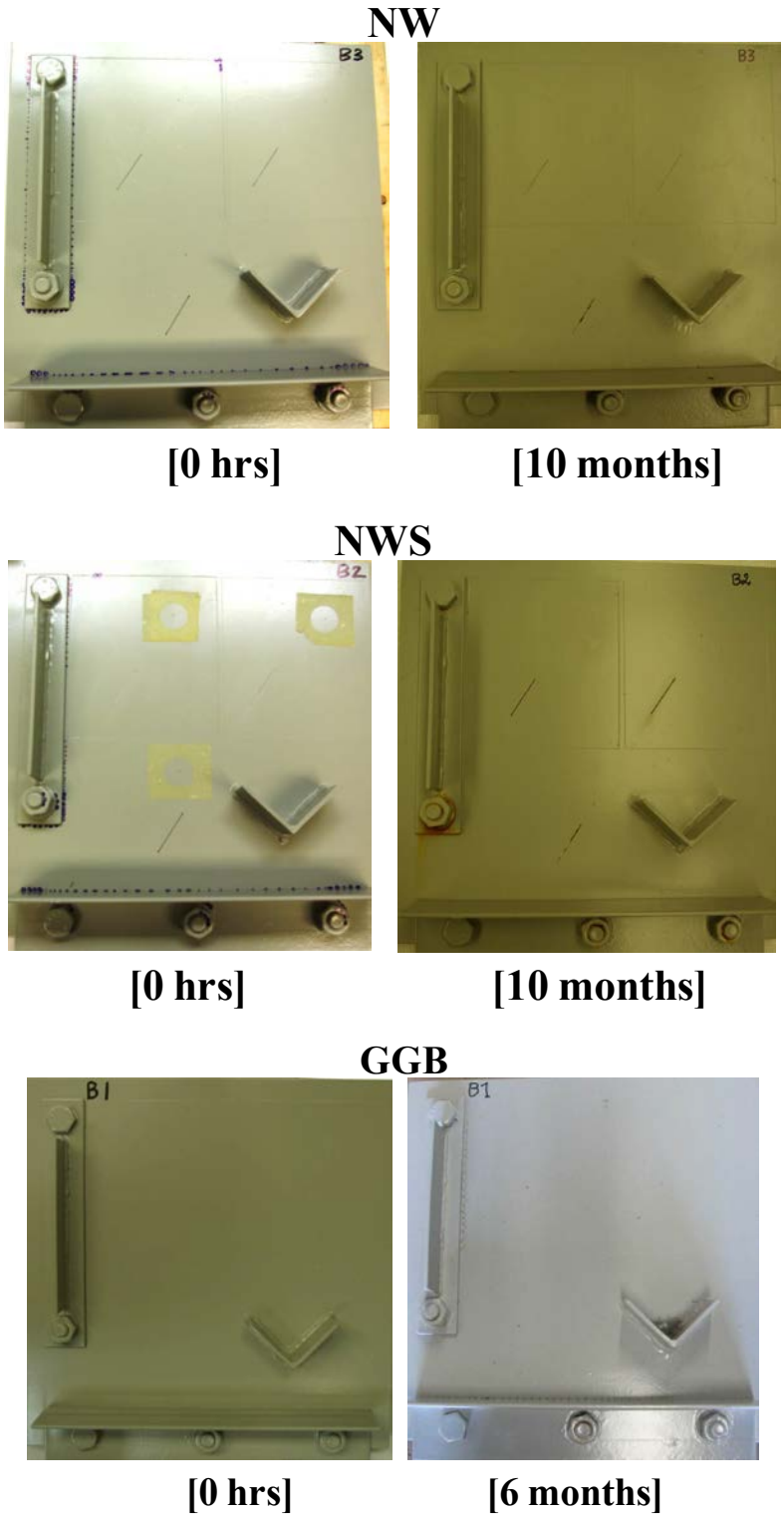

Figure 34. Photo. Progressive changes of ZE/E/PU—type II in NW, NWS, and GGB.

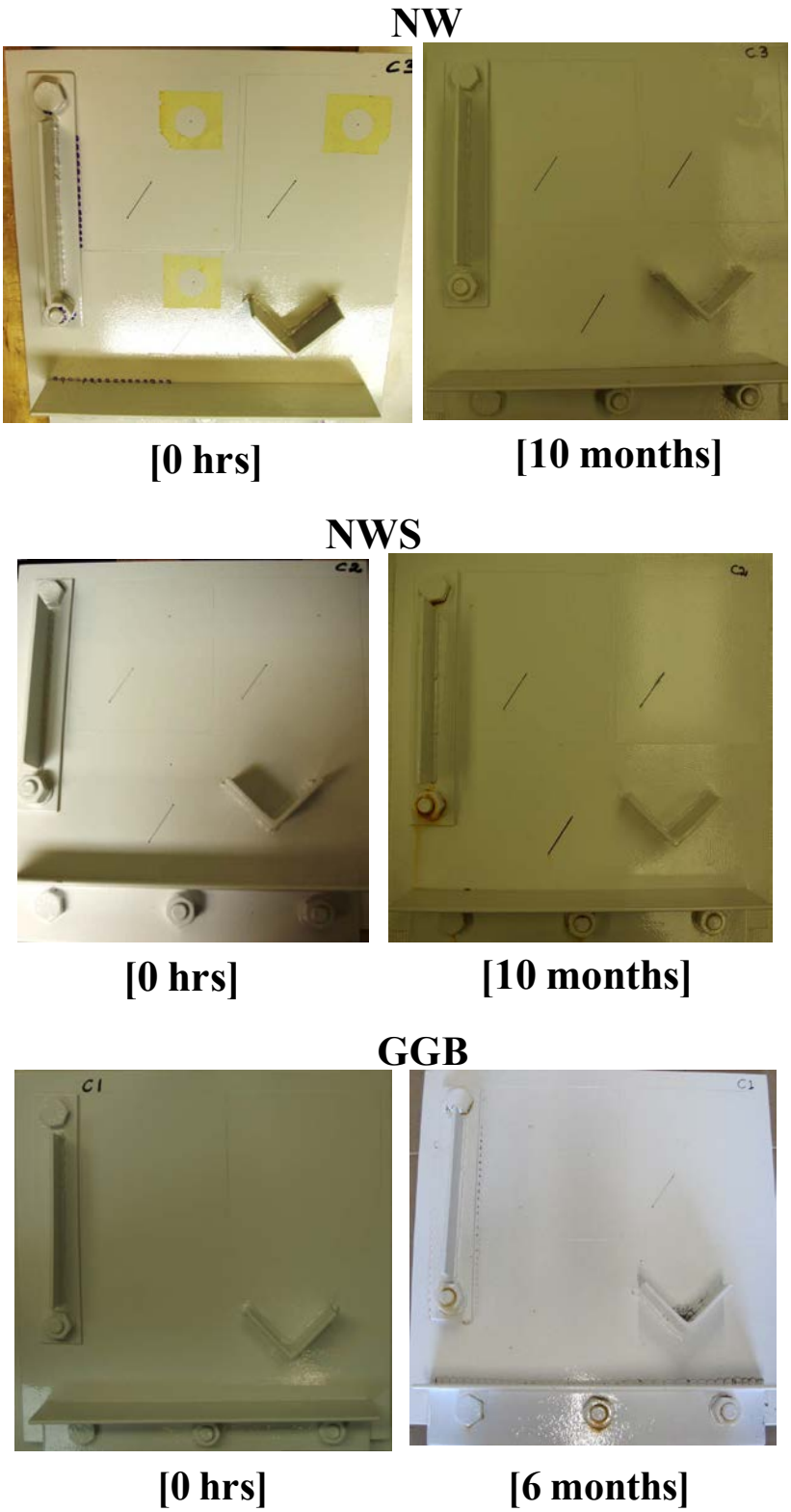

Figure 35. Photo. Progressive changes of MCU/E/F—type II in NW, NWS, and GGB.

NW

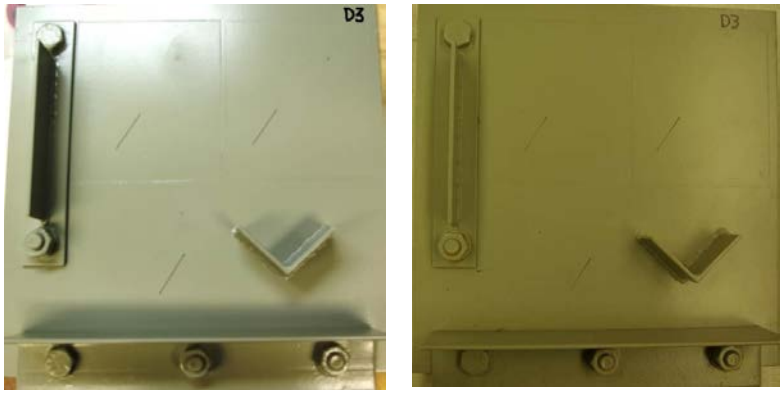

[0 hrs] [10 months]

NWS

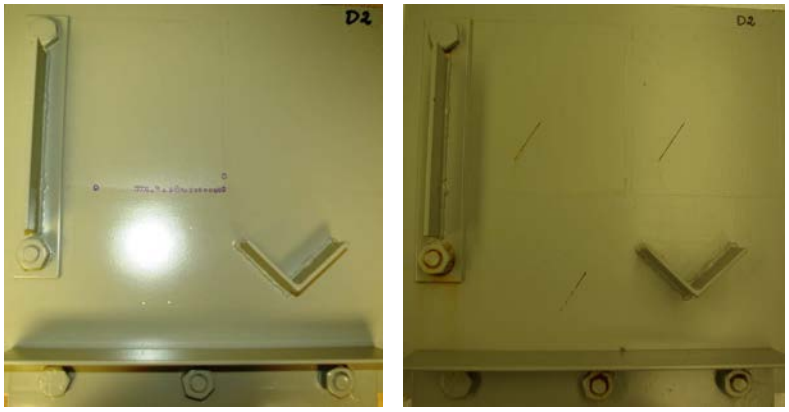

[0 hrs] [10 months]

GGB

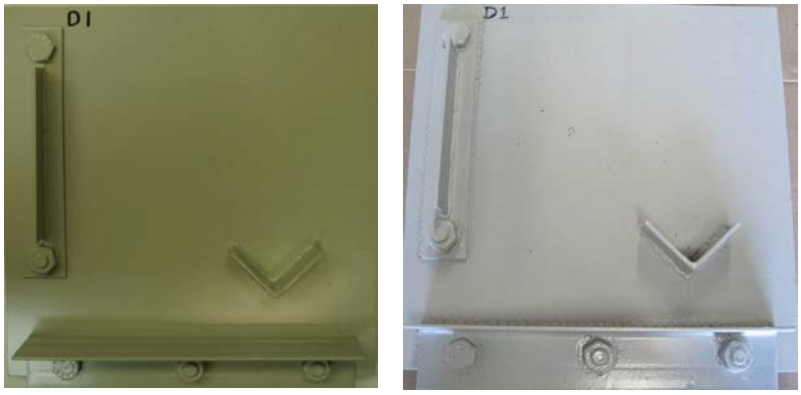

[0 hrs] [6 months]

Figure 36. Photo. Progressive changes of ZE/PU—type II in NW, NWS, and GGB.

NW

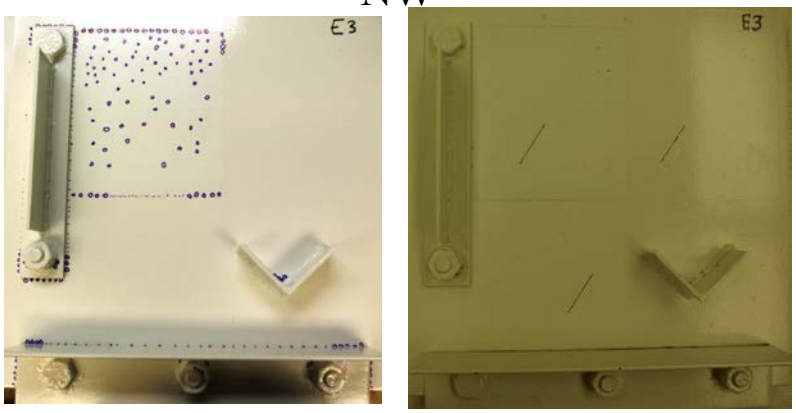

[0 hrs] **[10 months]**

NWS

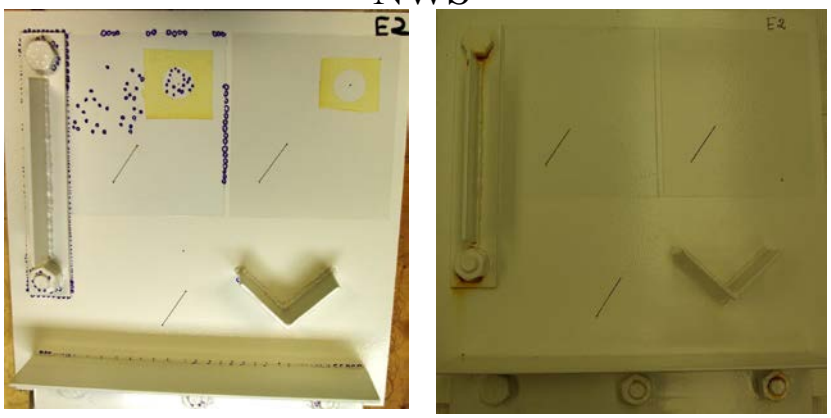

[0 hrs] **[10 months]**

GGB

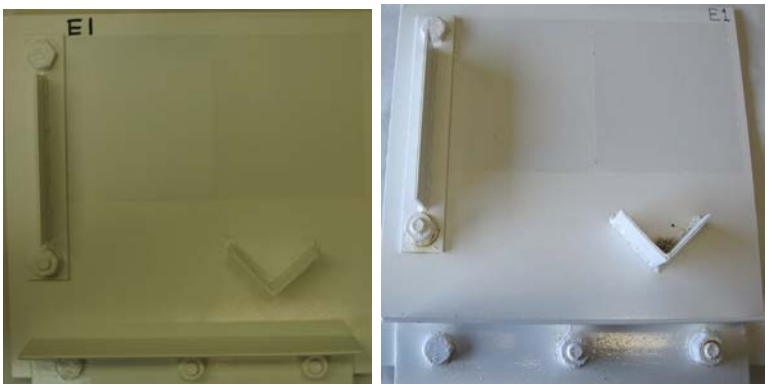

[0 hrs] **[6 months]**

Figure 37. Photo. Progressive changes of Zn/PS—type II in NW, NWS, and GGB.

NW

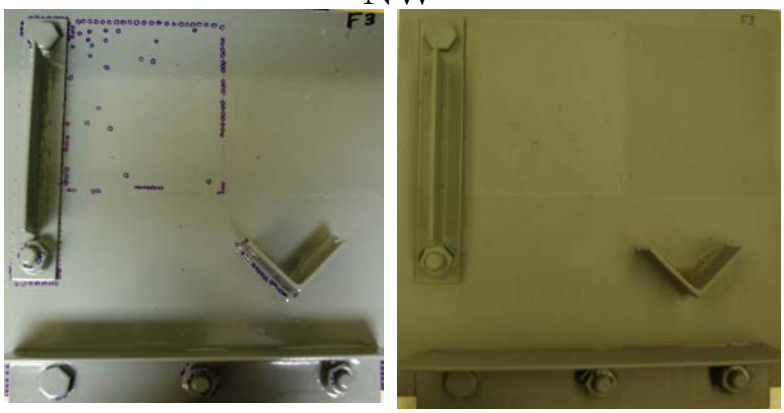

[0 hrs] **[10 months]**

NWS

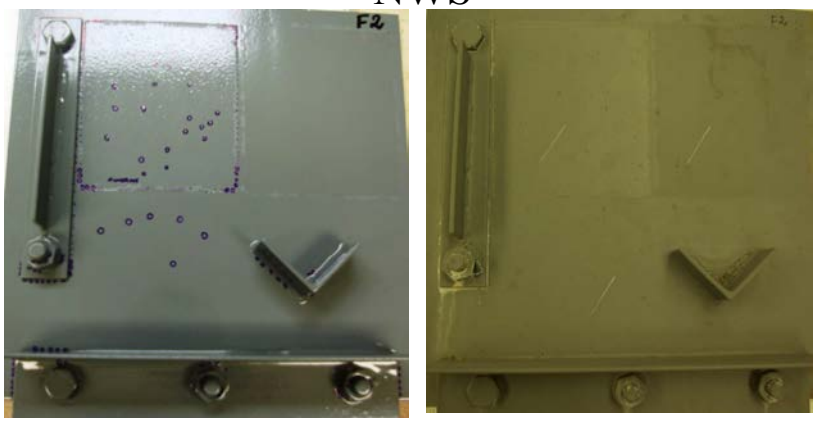

[0 hrs] **[10 months]**

GGB

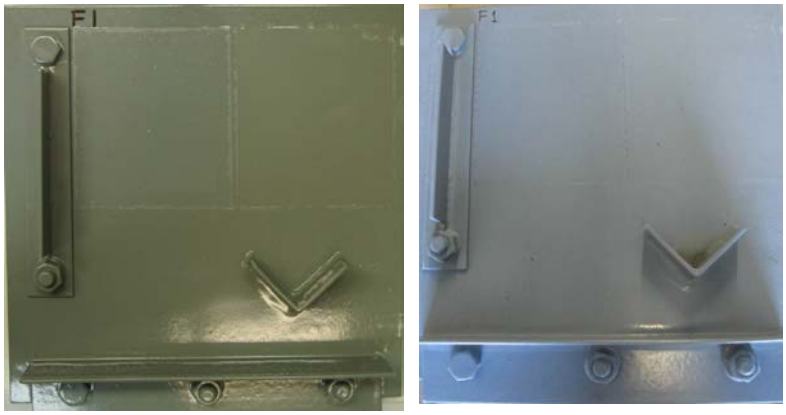

[0 hrs] **[6 months]**

Figure 38. Photo. Progressive changes of TSZ/LE—type II in NW, NWS, and GGB.

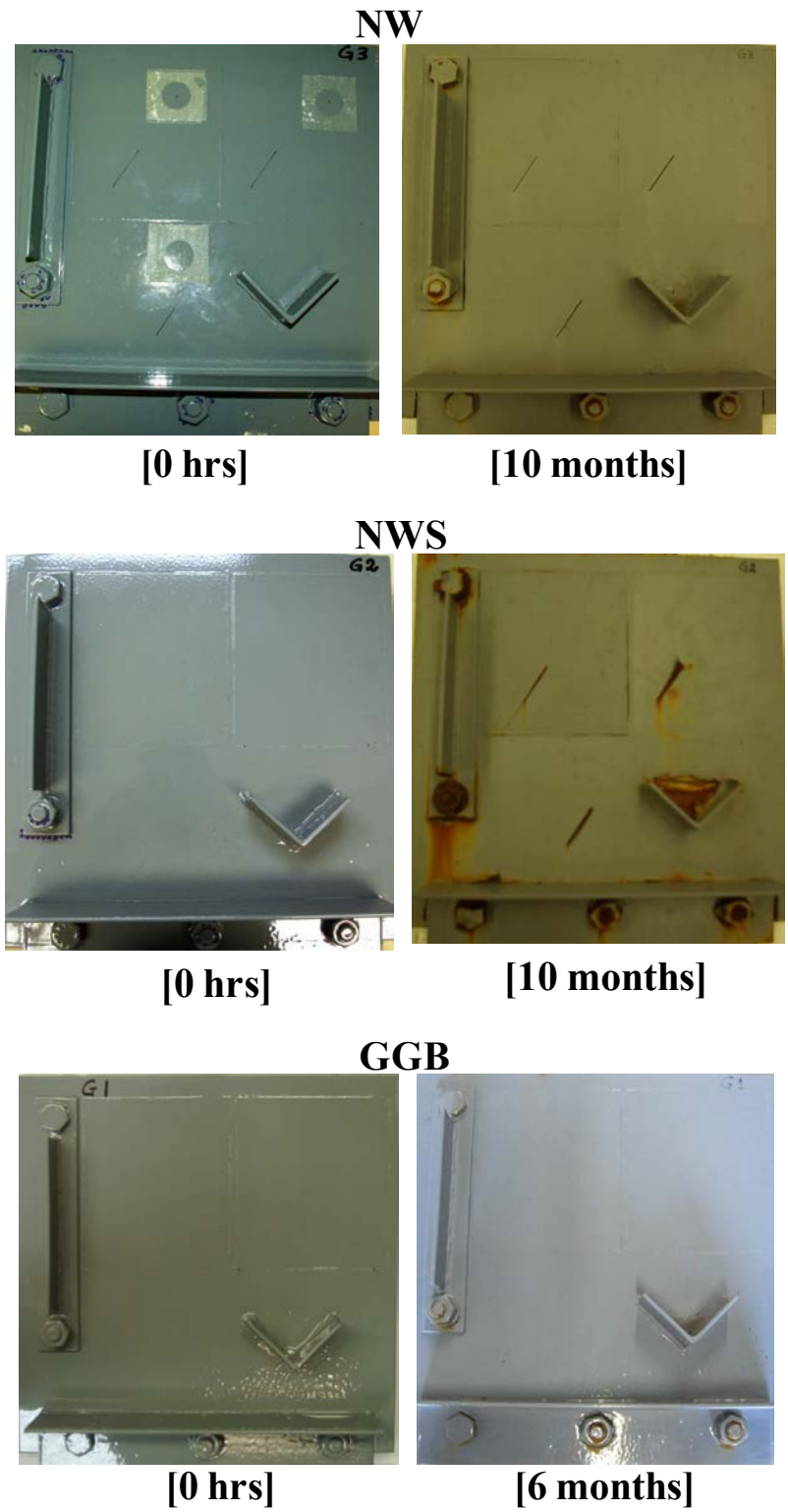

Figure 39. Photo. Progressive changes of ZnE/LE—type II in NW, NWS, and GGB.

NW

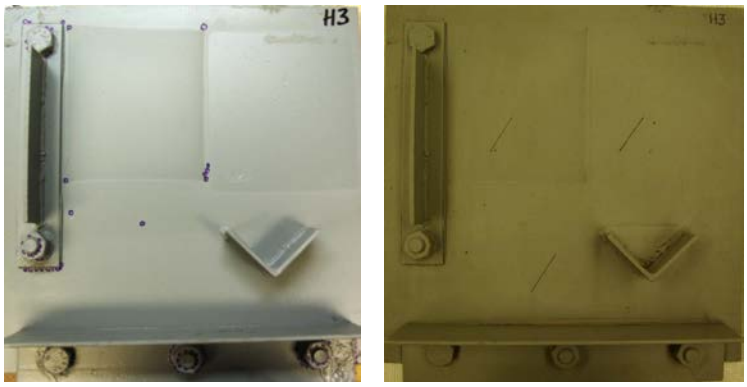

[0 hrs] **[10 months]**

NWS

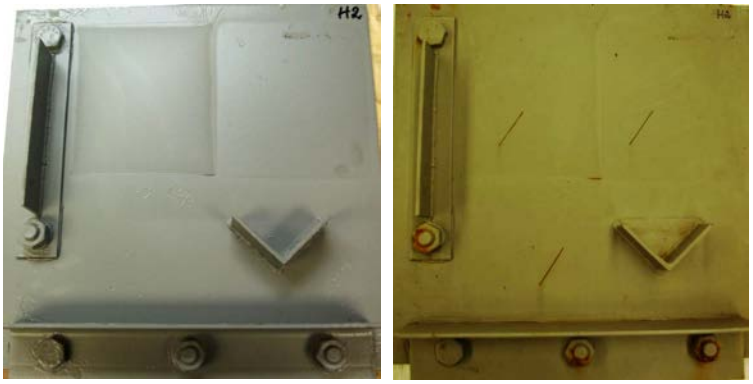

[0 hrs] **[10 months]**

GGB

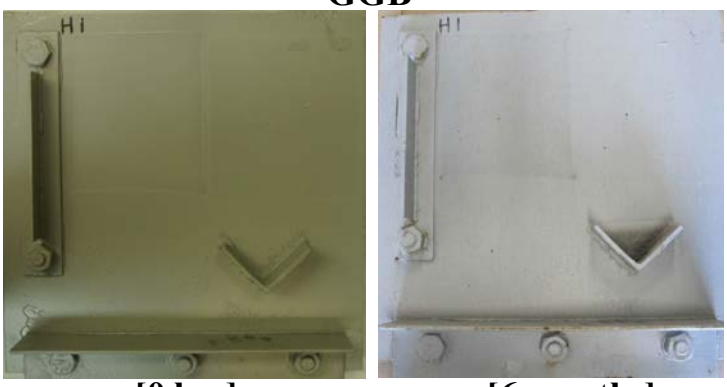

[0 hrs] **[6 months]**

Figure 40. Photo. Progressive changes of HRCSA—type II in NW, NWS, and GGB.

CHAPTER 4. CONCLUSIONS

The following conclusions are based on test results of the eight coating systems collected during the initial coating characterization, 3,600 h of ALT, 10 months of NW and NWS exposure testing, and 6 months of outdoor exposure testing at GGB:

- Test results from this study indicate that none of the selected coating systems, including the two three-coat control coatings, will provide maintenance-free corrosion protection to steel bridge structures for 100 years.

- The two three-coat control systems, IOZ/E/PU and ZE/E/PU, and the one-coat system, HRCSA, were chosen for their good performance records in an earlier FHWA one-coat study.[22] As expected, they performed well, and they were better than the other test coating systems in every category. The remaining five coating systems, ZE/PU, Zn/PS, TSZ/LE, ZnE/LE, and HRCSA, were selected for a possibility of providing superior performance to commercially available products in the current market. However, they did not deliver desirable performance exceeding the three best coating systems.

- Premature failure of two two-coat systems, TSZ/LE and ZnE/LE, was not anticipated during the coating selection process. Their performance was the worst among the eight coating systems and had a negative impact on this study, leading to early termination of the research. Three test coating systems, MCU/E/F, ZE/PU, and Zn/PS, performed satisfactorily in some categories and poorly in the others compared to the best performers. None of them showed consistently good performance.

- It is apparent that cutting-edge coating technology, regardless of cost, is not ready to deliver super durable coating systems that can last more than 100 years without significant maintenance interventions.

- Until future research and development efforts produce coating systems with extended service life, the main goal should be to use the proven legacy coating systems correctly by reducing human errors and improper applications. At the same time, researchers should strive to develop surface-tolerant primers against salts residue, adhered rusts, and mill scale; a simple yet reliable in situ test method for surface chloride concentration; and allowable chloride contamination(s) on the blasted steel surface. Significant advancement in these areas will allow for the creation of more durable steel bridge coatings than what is currently available.

REFERENCES

1. Kogler, B. (2008). "Managing the Infrastructure: The Role of Cost Knowledge," *Journal of Protective Coatings and Linings*, 22–31.

2. Kline, E.S. (2008). "Steel Bridges: Corrosion Protection for 100 Years," *Journal of Protective Coatings and Linings*, 20–31.

3. Appleman, B.R. and Kline, E.S. (2003). *Analysis of Cost for Shop Painting of Bridge*, KTA-Tator Report to FHWA.

4. Chong, S.L. and Yao, Y. (2000). *Laboratory and Test-Site Testing of Moisture-Cured Urethanes on Steel in Salt-rich Environment*, Report No. FHWA-RD-00-156, Federal Highway Administration, Washington, DC.

5. Chong, S.L. and Yao, Y. (2006). "Performance of Testing of Two-Coat Zinc-Rich Systems on Steel Bridges," *Journal of Protective Coatings and Linings*, 72–83.

6. Lee, S.K., Chong, S.L., and Yao, Y. (2006). *Performance Evaluation of Bridge Overcoating Materials Using Electrochemical Impedance Spectroscopy*, Proceedings of Paint and Coatings Expo, Tampa, FL.

7. Chong, S.L. and Yao, Y. (2006). "Selecting Overcoats For Bridges," *Public Roads*, *71*(2).

8. Lee, S.K., Kogler, B., and Yao, Y. (2010). *Outdoor Performance of One-Coat Systems Applicable to New Steel Bridges*, Proceeding of Paint and Coatings Expo, Phoenix, AZ.

9. Chong, S.L. and Yao, Y. (2006). "Are Two Coat as Effective as Three?," *Public Roads*, *70*(2).

10. Society for Protective Coatings. (2007). *Joint Surface Preparation Standard SSPC-SP5/NACE No.1: White Metal Blast Cleaning*, Pittsburgh, PA.

11. ASTM D1654-08. (2008). "Standard Test Method for Evaluation of Painted or Coated Specimens Subjected to Corrosive Environments," *ASTM Book of Standards Volume 06.01*, ASTM International, West Conshohocken, PA.

12. ASTM G85-11. (2011). "Standard Practice for Modified Salt Spray (Fog) Testing," *ASTM Book of Standards Volume 06.01*, ASTM International, West Conshohocken, PA.

13. Society for Protective Coatings. (2009). *SSPC-PA2: Measurement of Dry Coat Thickness with Magnetic Gages*, Pittsburgh, PA.

14. Nadal, M.E. (2001). "NIST Reference Goniophotometer for Specular Gloss Measurements," *Journal of Coatings Technology*, *73*(917), 73–80.

15. ASTM D523-08. (2008). "Standard Test Method for Specular Gloss," *ASTM Book of Standards Volume 06.01*, ASTM International, West Conshohocken, PA.

16. ASTM D2244-05. (2005). "Standard Practice for Calculation of Color Tolerances and Color Differences from Instrumentally Measured Color Coordinates," *ASTM Book of Standards Volume 06.01*, ASTM International, West Conshohocken, PA.

17. ASTM D4541-09e1. (2009). "Standard Test Method for Pull-Off Strength of Coatings Using Portable Adhesion Testers," *ASTM Book of Standards Volume 06.02*, ASTM International, West Conshohocken, PA.

18. ASTM G62-07. (2009). "Standard Test Methods for Holiday Detection in Pipeline Coatings (Method A)," *ASTM Book of Standards Volume 06.02*, ASTM International, West Conshohocken, PA.

19. ASTM D714-02. (2009). "Standard Test Method for Evaluating Degree of Blistering of Paints," *ASTM Book of Standards Volume 06.01*, ASTM International, West Conshohocken, PA.

20. ASTM D610-01. (2009)."Standard Test Method for Evaluating Degree of Rusting on Painted Steel Surfaces," *ASTM Book of Standards Volume 06.01*, ASTM International, West Conshohocken, PA.

21. ASTM D7087-05a. (2005). "Standard Test Method for An Imaging Technique to Measure Rust Creepage at Scribe on Coated Test Panels Subjected to Corrosive Environments," *ASTM Book of Standards Volume 06.01*, ASTM International, West Conshohocken, PA.

22. Yao, Y., Kodumuri, P., and Lee, S.K. (2011). *Performance Evaluation of One-Coat Systems for New Steel Bridges*, FHWA Report No. FHWA-HRT-11-046, Federal Highway Administration, Washington, DC.

HRDI-60/11-12(WEB)E